IEEE Access
Multidisciplinary ⋮ Rapid Review ⋮ Open Access Journal

Received 18 August 2022, accepted 10 October 2022, date of publication 17 October 2022, date of current version 26 October 2022.

Digital Object Identifier 10.1109/ACCESS.2022.3215250

RESEARCH ARTICLE

# Dual CUSUM Charts for Monitoring Autocorrelated AR (1) Processes Mean With s-Skipping Sampling Scheme

**YI LI[1], TAHIR MUNIR[1,2], AND XUELONG HU[3]**

[1]School of Statistics, Shanxi University of Finance and Economics, Taiyuan, Shanxi 030012, China
[2]Department of Anaesthesiology, The Aga Khan University, Karachi 74800, Pakistan
[3]School of Management, Nanjing University of Posts and Telecommunications, Nanjing 210049, China

Corresponding author: Tahir Munir (tahirmunir677@yahoo.com)

This work was supported in part by the Scientific Activities of Selected Returned Overseas Professionals in Shanxi Province under Grant 20220025, in part by the National Statistical Science Research Project of China under Grant 2022LZ14, in part by the Humanities and Social Sciences Foundation of Ministry of Education, China, under Grant 20YJA910004, and in part by the Shanxi Province Youth Talent Support Program under Grant 20190705.

**ABSTRACT** In statistical process monitoring, it is often assumed that the sequential observations generated by processes are independent and identically distributed (iid). However, in real practice, these observations tend to exhibit an autocorrelation pattern. Thus, an autocorrelated process yields misleading results in terms of a high false alarm rate and slow detection of process changes if employing iid-based designed monitoring schemes. Therefore, in this article, we propose the dual cumulative sum (DCUSUM) and dual Crosier's CUSUM (DCCUSUM) mean charts for monitoring the autocorrelated processes using a first-order autoregressive model. Monte Carlo simulations are extensively used to compute the performance measures: the average run length, standard deviation run length, extra quadratic loss, and relative average run length of the two-sided DCUSUM and DCCUSUM charts under both the zero-state and steady state cases. It is observed that as the level of autocorrelation increases, the performance of the studied charts deteriorates. Thus, a s-skipping sampling scheme is incorporated to reduce the negative effect of autocorrelation. To demonstrate the effect of autocorrelation and highlight implications further, a simulated dataset with a shift in the process mean is considered.

**INDEX TERMS** AR (1) model, autocorrelation, DCUSUM chart, Monte-Carlo simulations, s-skipping sampling, statistical process control.

## I. INTRODUCTION

Control charts (CCs) are commonly used in statistical process control (SPC) to keep a check on industrial and service processes in order to improve process quality and productivity. The main objective of a CC is to distinguish between two types of variability: random and assignable causes. A process is said to be in-control (IC) if it only operates with a random cause of variation. On the other hand, the process is out-of-control (OC) when it continues to operate in the presence of identifiable causes (as a result of additional variations brought on by equipment, human error, and/or material error). Any efficient monitoring technique must react quickly to changes in parameter(s) of interest in order to eliminate/reduce undesirable waste (cf., Montgomery, [1]).

CCs are classified into two categories based on their current and previous realizations, namely: memory-less and memory-type. In the former category, the most well-known and easiest-to-implement SPC schemes are those developed by CC pioneer Dr. Walter A. Shewhart [2] in the 1920s. Despite their simplicity and excellent adaptability for large shifts, they have a major drawback in noticing slight to moderate shifts. Page [3] and Roberts [4], on the other hand, proposed memory-type charts, primarily cumulative sum (CUSUM) and exponentially weighted moving average (EWMA), respectively. Later, Crosier [5] proposed a modified CUSUM chart for detecting mean shifts, known as the CCUSUM chart. The functioning of the CCUSUM chart is

The associate editor coordinating the review of this manuscript and approving it for publication was Nikhil Padhi.

**TABLE 1.** Zero-state $ARL_1$ profile of the DCUSUM chart with $ARL_0 = 500$.

| δ↓ | S↓ | ϕ→ | 0.0 | 0.1 | 0.2 | 0.3 | 0.4 | 0.5 | 0.6 | 0.7 | 0.8 | 0.9 |
|---|---|---|---|---|---|---|---|---|---|---|---|---|
| 0.20 | 0 | ARL | 271.37 | 293.38 | 313.85 | 332.24 | 353.39 | 368.79 | 384.34 | 397.44 | 412.6 | 422.86 |
| | | SDRL | 267.01 | 291.66 | 309.25 | 328.87 | 349.26 | 364.56 | 382.44 | 397.42 | 410.55 | 419.41 |
| | 1 | ARL | 273.3 | 275.04 | 281.42 | 292.88 | 307.55 | 323.54 | 344.64 | 367.1 | 390.4 | 412.35 |
| | | SDRL | 269.66 | 271.58 | 277.03 | 290.39 | 305.28 | 321.18 | 341.5 | 362.65 | 385.21 | 408.61 |
| | 2 | ARL | 272.05 | 272.67 | 274.85 | 277.56 | 287.44 | 299.31 | 318.85 | 340.8 | 371.22 | 403.41 |
| | | SDRL | 267.76 | 268.15 | 272.78 | 272.87 | 284 | 295.58 | 314.85 | 336.74 | 368.1 | 399.89 |
| | 3 | ARL | 273.88 | 272.32 | 273.08 | 274.05 | 278.94 | 284.39 | 299.51 | 321.85 | 353.48 | 393.07 |
| | | SDRL | 271.69 | 268.74 | 269.5 | 269.94 | 276.55 | 279.98 | 295.98 | 317.36 | 349.03 | 389.78 |
| 0.40 | 0 | ARL | 96.32 | 112.83 | 131.4 | 150.02 | 170.4 | 191.96 | 213.6 | 236.89 | 259.46 | 279.97 |
| | | SDRL | 92.01 | 108.75 | 127.7 | 145.38 | 166.57 | 188.25 | 210.19 | 233.13 | 255.82 | 276.88 |
| | 1 | ARL | 96.65 | 98.22 | 102.66 | 111.45 | 123.92 | 140.82 | 162.68 | 190.02 | 222.91 | 261.3 |
| | | SDRL | 92.75 | 93.58 | 98.56 | 107.11 | 119.69 | 136.78 | 158.39 | 186.58 | 218.42 | 258.41 |
| | 2 | ARL | 96.16 | 96.72 | 97.88 | 100.71 | 106.97 | 117.44 | 134.26 | 158.73 | 194.56 | 242.77 |
| | | SDRL | 92 | 92.09 | 93.98 | 96.79 | 103.35 | 113.45 | 130.14 | 154.93 | 190.88 | 239.69 |
| | 3 | ARL | 96.13 | 95.98 | 96.78 | 97.39 | 100.56 | 106.68 | 117.88 | 138.29 | 172.1 | 226.72 |
| | | SDRL | 92.01 | 91.79 | 92.76 | 92.99 | 95.77 | 102.42 | 113.61 | 134.72 | 168.7 | 223.39 |
| 0.60 | 0 | ARL | 38.93 | 47.05 | 56.62 | 67.8 | 80.83 | 96.01 | 111.62 | 130.35 | 150.17 | 169.72 |
| | | SDRL | 34.49 | 42.4 | 51.87 | 63.63 | 77.07 | 91.84 | 107.3 | 126.46 | 146.01 | 165.7 |
| | 1 | ARL | 39.01 | 39.52 | 42.07 | 46.23 | 52.38 | 62.04 | 75.47 | 93.48 | 118.96 | 151.89 |
| | | SDRL | 34.39 | 35.06 | 37.57 | 41.68 | 47.83 | 57.57 | 71.04 | 89.16 | 114.91 | 148.36 |
| | 2 | ARL | 38.88 | 39.01 | 39.46 | 40.97 | 43.76 | 49.35 | 58.35 | 73.04 | 97.21 | 135.73 |
| | | SDRL | 34.36 | 34.43 | 34.89 | 36.6 | 39.11 | 44.77 | 53.72 | 68.69 | 92.83 | 131.28 |
| | 3 | ARL | 38.87 | 38.84 | 38.83 | 39.37 | 40.75 | 43.69 | 49.72 | 61.26 | 82.04 | 121.74 |
| | | SDRL | 34.38 | 34.3 | 34.34 | 34.81 | 36.14 | 39.07 | 44.99 | 56.59 | 77.83 | 116.93 |
| 0.80 | 0 | ARL | 19.55 | 23.65 | 28.46 | 34.58 | 41.84 | 51.02 | 60.98 | 73.07 | 87.33 | 102.87 |
| | | SDRL | 15.17 | 19.31 | 24.05 | 30.12 | 37.39 | 46.34 | 56.3 | 68.86 | 82.85 | 98.87 |
| | 1 | ARL | 19.56 | 20 | 21.06 | 23.22 | 26.52 | 31.48 | 38.88 | 50.04 | 65.94 | 89.1 |
| | | SDRL | 15.25 | 15.8 | 16.65 | 18.81 | 22.06 | 26.95 | 34.33 | 45.48 | 61.53 | 84.76 |
| | 2 | ARL | 19.53 | 19.57 | 19.82 | 20.53 | 22.04 | 24.7 | 29.49 | 37.6 | 51.96 | 76.94 |
| | | SDRL | 15.19 | 15.29 | 15.43 | 16.2 | 17.64 | 20.26 | 25.01 | 33.09 | 47.47 | 72.36 |
| | 3 | ARL | 19.54 | 19.5 | 19.64 | 19.82 | 20.53 | 21.98 | 24.93 | 30.64 | 42.72 | 67.72 |
| | | SDRL | 15.23 | 15.2 | 15.21 | 15.52 | 16.16 | 17.58 | 20.49 | 26.12 | 38.26 | 63.09 |
| 1.00 | 0 | ARL | 11.92 | 14.18 | 16.9 | 20.36 | 24.54 | 29.71 | 36.1 | 43.84 | 53.29 | 63.83 |
| | | SDRL | 8.03 | 10.11 | 12.64 | 16.1 | 20.12 | 25.2 | 31.73 | 39.18 | 48.94 | 59.28 |
| | 1 | ARL | 11.92 | 12.12 | 12.75 | 13.95 | 15.67 | 18.57 | 22.78 | 29.22 | 39.35 | 54.16 |
| | | SDRL | 8.09 | 8.22 | 8.83 | 9.87 | 11.53 | 14.27 | 18.33 | 24.66 | 34.72 | 50.02 |
| | 2 | ARL | 11.88 | 11.85 | 12.06 | 12.49 | 13.31 | 14.78 | 17.36 | 22.1 | 30.44 | 46.6 |
| | | SDRL | 8.01 | 7.95 | 8.1 | 8.5 | 9.27 | 10.68 | 13.08 | 17.77 | 25.84 | 41.9 |
| | 3 | ARL | 11.93 | 11.95 | 11.95 | 12.09 | 12.43 | 13.23 | 14.85 | 18.23 | 25.03 | 40.39 |
| | | SDRL | 8.03 | 8.04 | 8.06 | 8.17 | 8.48 | 9.24 | 10.73 | 13.96 | 20.51 | 35.89 |
| 1.20 | 0 | ARL | 8.31 | 9.66 | 11.34 | 13.41 | 16.01 | 19.33 | 23.3 | 28.27 | 34.84 | 41.82 |
| | | SDRL | 4.89 | 6.02 | 7.48 | 9.37 | 11.85 | 15.07 | 18.88 | 23.72 | 30.4 | 37.39 |
| | 1 | ARL | 8.3 | 8.45 | 8.85 | 9.51 | 10.65 | 12.36 | 14.99 | 18.92 | 25.23 | 35.15 |
| | | SDRL | 4.85 | 5 | 5.32 | 5.87 | 6.9 | 8.41 | 10.89 | 14.63 | 20.84 | 30.58 |
| | 2 | ARL | 8.31 | 8.33 | 8.41 | 8.67 | 9.14 | 10.07 | 11.67 | 14.49 | 19.78 | 30.12 |
| | | SDRL | 4.88 | 4.89 | 4.96 | 5.17 | 5.56 | 6.38 | 7.79 | 10.38 | 15.49 | 25.65 |
| | 3 | ARL | 8.31 | 8.32 | 8.33 | 8.42 | 8.62 | 9.14 | 10.16 | 12.13 | 16.38 | 26.04 |
| | | SDRL | 4.88 | 4.9 | 4.91 | 4.96 | 5.15 | 5.57 | 6.46 | 8.21 | 12.17 | 21.58 |
| 1.40 | 0 | ARL | 6.3 | 7.22 | 8.39 | 9.76 | 11.53 | 13.66 | 16.38 | 19.77 | 23.82 | 28.85 |
| | | SDRL | 3.31 | 3.99 | 4.96 | 6.11 | 7.68 | 9.66 | 12.19 | 15.43 | 19.39 | 24.33 |
| | 1 | ARL | 6.28 | 6.39 | 6.64 | 7.15 | 7.89 | 9.03 | 10.74 | 13.42 | 17.63 | 24.41 |
| | | SDRL | 3.29 | 3.38 | 3.54 | 3.95 | 4.51 | 5.47 | 6.92 | 9.41 | 13.43 | 20.07 |
| | 2 | ARL | 6.3 | 6.32 | 6.35 | 6.56 | 6.88 | 7.5 | 8.6 | 10.48 | 13.94 | 20.74 |
| | | SDRL | 3.32 | 3.32 | 3.36 | 3.51 | 3.73 | 4.24 | 5.12 | 6.75 | 9.87 | 16.32 |
| | 3 | ARL | 6.28 | 6.3 | 6.34 | 6.38 | 6.53 | 6.85 | 7.56 | 8.91 | 11.71 | 18.15 |
| | | SDRL | 3.3 | 3.32 | 3.33 | 3.36 | 3.47 | 3.74 | 4.29 | 5.36 | 7.83 | 13.82 |

**TABLE 1.** *(Continued.)* Zero-state $ARL_1$ profile of the DCUSUM chart with $ARL_0 = 500$.

| | | | | | | | | | | | | |
|---|---|---|---|---|---|---|---|---|---|---|---|---|
| 1.60 | 0 | ARL | 5.05 | 5.77 | 6.58 | 7.58 | 8.82 | 10.35 | 12.21 | 14.54 | 17.44 | 21.02 |
| | | SDRL | 2.43 | 2.93 | 3.53 | 4.31 | 5.3 | 6.66 | 8.29 | 10.48 | 13.21 | 16.71 |
| | 1 | ARL | 5.06 | 5.12 | 5.32 | 5.67 | 6.22 | 7.06 | 8.33 | 10.12 | 13.1 | 17.75 |
| | | SDRL | 2.45 | 2.48 | 2.62 | 2.86 | 3.25 | 3.88 | 4.9 | 6.39 | 9.14 | 13.51 |
| | 2 | ARL | 5.05 | 5.05 | 5.11 | 5.22 | 5.48 | 5.95 | 6.71 | 8.07 | 10.47 | 15.33 |
| | | SDRL | 2.45 | 2.43 | 2.47 | 2.56 | 2.72 | 3.07 | 3.62 | 4.69 | 6.73 | 11.21 |
| | 3 | ARL | 5.06 | 5.05 | 5.07 | 5.1 | 5.21 | 5.49 | 5.99 | 6.97 | 8.97 | 13.5 |
| | | SDRL | 2.44 | 2.44 | 2.46 | 2.48 | 2.55 | 2.73 | 3.09 | 3.8 | 5.43 | 9.48 |
| 1.80 | 0 | ARL | 4.2 | 4.76 | 5.4 | 6.18 | 7.08 | 8.22 | 9.61 | 11.33 | 13.47 | 15.99 |
| | | SDRL | 1.92 | 2.24 | 2.67 | 3.22 | 3.92 | 4.78 | 5.99 | 7.52 | 9.41 | 11.83 |
| | 1 | ARL | 4.2 | 4.25 | 4.4 | 4.69 | 5.11 | 5.78 | 6.69 | 8.08 | 10.22 | 13.65 |
| | | SDRL | 1.9 | 1.95 | 2.02 | 2.2 | 2.48 | 2.94 | 3.6 | 4.7 | 6.51 | 9.56 |
| | 2 | ARL | 4.2 | 4.2 | 4.22 | 4.34 | 4.54 | 4.91 | 5.52 | 6.53 | 8.36 | 11.86 |
| | | SDRL | 1.9 | 1.92 | 1.94 | 2 | 2.12 | 2.34 | 2.75 | 3.47 | 4.93 | 7.95 |
| | 3 | ARL | 4.2 | 4.2 | 4.21 | 4.26 | 4.33 | 4.53 | 4.94 | 5.69 | 7.19 | 10.51 |
| | | SDRL | 1.92 | 1.91 | 1.92 | 1.96 | 1.99 | 2.11 | 2.37 | 2.86 | 3.98 | 6.73 |
| 2.00 | 0 | ARL | 3.59 | 4.03 | 4.56 | 5.18 | 5.91 | 6.8 | 7.85 | 9.16 | 10.78 | 12.77 |
| | | SDRL | 1.58 | 1.81 | 2.12 | 2.52 | 3.02 | 3.69 | 4.49 | 5.55 | 6.99 | 8.83 |
| | 1 | ARL | 3.59 | 3.62 | 3.75 | 3.99 | 4.35 | 4.85 | 5.61 | 6.67 | 8.36 | 10.96 |
| | | SDRL | 1.58 | 1.6 | 1.67 | 1.79 | 2 | 2.31 | 2.82 | 3.59 | 4.93 | 7.17 |
| | 2 | ARL | 3.58 | 3.58 | 3.6 | 3.71 | 3.88 | 4.16 | 4.66 | 5.47 | 6.91 | 9.57 |
| | | SDRL | 1.59 | 1.58 | 1.59 | 1.64 | 1.72 | 1.89 | 2.18 | 2.72 | 3.78 | 5.93 |
| | 3 | ARL | 3.59 | 3.58 | 3.6 | 3.61 | 3.69 | 3.86 | 4.19 | 4.8 | 5.98 | 8.54 |
| | | SDRL | 1.58 | 1.57 | 1.59 | 1.59 | 1.63 | 1.72 | 1.91 | 2.28 | 3.08 | 5.08 |

**TABLE 2.** Steady-state $ARL_1$ profile of the two-sided DCUSUM chart with $ARL_0 = 500$.

| δ↓ | S↓ | ϕ→ | 0.0 | 0.1 | 0.2 | 0.3 | 0.4 | 0.5 | 0.6 | 0.7 | 0.8 | 0.9 |
|---|---|---|---|---|---|---|---|---|---|---|---|---|
| 0.20 | 0 | ARL | 272.55 | 294.19 | 315.05 | 332.61 | 350.91 | 366.77 | 383.88 | 399.84 | 411.01 | 424.08 |
| | | SDRL | 271.12 | 293.47 | 315.29 | 332.17 | 348.86 | 365.48 | 383.85 | 400.35 | 412.01 | 424.32 |
| | 1 | ARL | 272.99 | 275.27 | 279.51 | 290.63 | 306.03 | 323.81 | 346.06 | 368.27 | 389.27 | 412.84 |
| | | SDRL | 271.74 | 273.64 | 277.73 | 291.38 | 305.48 | 321.92 | 344.38 | 366.87 | 391.96 | 416.30 |
| | 2 | ARL | 272.04 | 272.60 | 274.70 | 278.56 | 286.58 | 300.94 | 317.24 | 342.01 | 370.35 | 403.02 |
| | | SDRL | 270.42 | 270.75 | 274.22 | 276.90 | 286.13 | 299.98 | 318.20 | 341.72 | 368.69 | 400.97 |
| | 3 | ARL | 271.64 | 271.26 | 272.83 | 274.29 | 277.36 | 286.55 | 300.84 | 322.57 | 353.24 | 393.00 |
| | | SDRL | 270.07 | 269.68 | 271.30 | 274.34 | 275.49 | 284.91 | 299.24 | 320.75 | 351.51 | 393.20 |
| 0.40 | 0 | ARL | 95.73 | 112.23 | 129.82 | 149.61 | 169.34 | 191.51 | 213.86 | 236.97 | 256.87 | 280.86 |
| | | SDRL | 93.18 | 109.63 | 126.69 | 146.46 | 167.00 | 188.62 | 211.32 | 235.89 | 254.88 | 279.98 |
| | 1 | ARL | 95.42 | 96.93 | 101.73 | 110.35 | 122.98 | 139.35 | 161.86 | 188.51 | 223.39 | 261.34 |
| | | SDRL | 92.12 | 93.69 | 98.78 | 107.31 | 120.34 | 137.30 | 159.16 | 186.79 | 223.14 | 261.09 |
| | 2 | ARL | 96.10 | 95.76 | 96.77 | 99.74 | 105.85 | 116.16 | 132.66 | 157.94 | 194.01 | 244.32 |
| | | SDRL | 93.26 | 92.37 | 94.02 | 96.98 | 103.24 | 113.86 | 130.36 | 155.48 | 190.98 | 242.09 |
| | 3 | ARL | 96.31 | 95.61 | 95.85 | 96.98 | 99.51 | 105.62 | 116.93 | 137.01 | 172.00 | 227.04 |
| | | SDRL | 93.45 | 92.54 | 92.91 | 94.11 | 96.68 | 102.91 | 114.27 | 134.12 | 169.99 | 225.26 |
| 0.60 | 0 | ARL | 37.88 | 46.51 | 55.75 | 67.16 | 79.55 | 94.60 | 111.20 | 128.35 | 148.31 | 169.85 |
| | | SDRL | 34.11 | 43.15 | 52.28 | 63.84 | 75.99 | 91.43 | 108.64 | 125.62 | 146.34 | 166.99 |
| | 1 | ARL | 38.11 | 38.88 | 40.96 | 45.34 | 51.98 | 61.28 | 74.58 | 93.36 | 118.19 | 151.00 |
| | | SDRL | 34.47 | 35.21 | 37.37 | 41.60 | 48.12 | 57.74 | 71.33 | 90.50 | 115.65 | 149.43 |
| | 2 | ARL | 38.29 | 38.14 | 38.79 | 40.10 | 43.25 | 48.58 | 57.45 | 72.67 | 96.77 | 134.48 |
| | | SDRL | 34.64 | 34.44 | 35.21 | 36.60 | 39.76 | 44.86 | 54.08 | 69.64 | 93.71 | 132.20 |
| | 3 | ARL | 37.94 | 38.01 | 38.28 | 38.60 | 40.06 | 43.18 | 48.91 | 59.95 | 81.52 | 120.93 |
| | | SDRL | 34.33 | 34.33 | 34.52 | 34.91 | 36.35 | 39.69 | 45.37 | 56.61 | 78.35 | 118.63 |
| | 0 | ARL | 19.00 | 22.95 | 27.93 | 33.89 | 40.94 | 49.86 | 60.22 | 72.67 | 86.12 | 101.61 |

**TABLE 2.** ***(Continued.)*** **Steady-state $ARL_1$ profile of the two-sided DCUSUM chart with $ARL_0 = 500$.**

| | | | | | | | | | | | | |
|---|---|---|---|---|---|---|---|---|---|---|---|---|
| 0.80 | | SDRL | 15.29 | 19.23 | 24.16 | 30.28 | 37.42 | 46.23 | 56.73 | 69.48 | 82.88 | 98.39 |
| | 1 | ARL | 19.08 | 19.30 | 20.57 | 22.54 | 25.80 | 30.82 | 38.15 | 49.17 | 65.03 | 88.43 |
| | | SDRL | 15.31 | 15.56 | 16.88 | 18.83 | 21.89 | 27.11 | 34.50 | 45.43 | 61.74 | 85.31 |
| | 2 | ARL | 19.00 | 19.04 | 19.23 | 19.98 | 21.48 | 24.15 | 28.72 | 36.75 | 50.85 | 75.91 |
| | | SDRL | 15.29 | 15.30 | 15.49 | 16.21 | 17.81 | 20.39 | 24.81 | 33.14 | 47.27 | 72.67 |
| | 3 | ARL | 18.97 | 19.03 | 19.09 | 19.30 | 19.85 | 21.41 | 24.42 | 30.13 | 41.89 | 67.06 |
| | | SDRL | 15.25 | 15.31 | 15.48 | 15.57 | 16.12 | 17.63 | 20.72 | 26.46 | 38.05 | 63.58 |
| 1.00 | 0 | ARL | 11.42 | 13.65 | 16.33 | 19.71 | 23.91 | 29.04 | 35.43 | 43.04 | 52.56 | 63.12 |
| | | SDRL | 8.00 | 10.07 | 12.66 | 16.02 | 20.21 | 25.37 | 31.62 | 39.70 | 49.24 | 59.59 |
| | 1 | ARL | 11.50 | 11.65 | 12.26 | 13.41 | 15.23 | 17.97 | 22.20 | 28.52 | 38.43 | 53.00 |
| | | SDRL | 8.08 | 8.25 | 8.76 | 9.85 | 11.57 | 14.21 | 18.43 | 24.86 | 34.77 | 49.45 |
| | 2 | ARL | 11.52 | 11.46 | 11.64 | 11.96 | 12.78 | 14.30 | 16.85 | 21.39 | 29.71 | 45.64 |
| | | SDRL | 8.08 | 8.01 | 8.24 | 8.53 | 9.31 | 10.74 | 13.27 | 17.69 | 25.75 | 41.97 |
| | 3 | ARL | 11.51 | 11.51 | 11.52 | 11.62 | 11.94 | 12.78 | 14.43 | 17.65 | 24.40 | 39.68 |
| | | SDRL | 8.02 | 8.08 | 8.10 | 8.17 | 8.45 | 9.29 | 10.91 | 13.90 | 20.65 | 36.14 |
| 1.20 | 0 | ARL | 7.94 | 9.30 | 10.93 | 12.93 | 15.55 | 18.80 | 22.65 | 27.66 | 33.89 | 41.14 |
| | | SDRL | 4.89 | 6.05 | 7.56 | 9.46 | 12.02 | 15.04 | 18.88 | 23.95 | 30.20 | 37.43 |
| | 1 | ARL | 7.93 | 8.06 | 8.45 | 9.14 | 10.18 | 11.92 | 14.42 | 18.45 | 24.59 | 34.30 |
| | | SDRL | 4.89 | 4.98 | 5.36 | 5.92 | 6.85 | 8.45 | 10.85 | 14.82 | 20.76 | 30.62 |
| | 2 | ARL | 7.96 | 7.95 | 8.02 | 8.26 | 8.79 | 9.67 | 11.21 | 13.92 | 19.22 | 29.19 |
| | | SDRL | 4.91 | 4.89 | 4.96 | 5.15 | 5.61 | 6.39 | 7.80 | 10.36 | 15.42 | 25.53 |
| | 3 | ARL | 7.96 | 7.93 | 7.94 | 8.03 | 8.27 | 8.78 | 9.73 | 11.65 | 15.79 | 25.35 |
| | | SDRL | 4.88 | 4.89 | 4.90 | 4.98 | 5.17 | 5.60 | 6.46 | 8.19 | 12.16 | 21.66 |
| 1.40 | 0 | ARL | 5.99 | 6.92 | 8.00 | 9.35 | 11.06 | 13.17 | 15.81 | 18.98 | 23.24 | 28.19 |
| | | SDRL | 3.31 | 4.05 | 4.91 | 6.14 | 7.64 | 9.65 | 12.14 | 15.28 | 19.42 | 24.55 |
| | 1 | ARL | 6.00 | 6.10 | 6.35 | 6.82 | 7.56 | 8.66 | 10.30 | 12.92 | 17.03 | 23.76 |
| | | SDRL | 3.30 | 3.38 | 3.60 | 3.95 | 4.57 | 5.50 | 6.94 | 9.33 | 13.40 | 20.10 |
| | 2 | ARL | 6.02 | 6.02 | 6.08 | 6.22 | 6.58 | 7.19 | 8.20 | 10.04 | 13.47 | 20.31 |
| | | SDRL | 3.33 | 3.33 | 3.37 | 3.48 | 3.78 | 4.26 | 5.08 | 6.76 | 9.95 | 16.52 |
| | 3 | ARL | 6.01 | 6.00 | 6.01 | 6.08 | 6.26 | 6.55 | 7.22 | 8.52 | 11.25 | 17.56 |
| | | SDRL | 3.31 | 3.31 | 3.32 | 3.38 | 3.51 | 3.74 | 4.29 | 5.38 | 7.86 | 13.92 |
| 1.60 | 0 | ARL | 4.80 | 5.48 | 6.27 | 7.23 | 8.42 | 9.92 | 11.70 | 14.02 | 16.90 | 20.45 |
| | | SDRL | 2.44 | 2.92 | 3.53 | 4.30 | 5.31 | 6.61 | 8.24 | 10.43 | 13.30 | 16.82 |
| | 1 | ARL | 4.80 | 4.87 | 5.07 | 5.42 | 5.93 | 6.75 | 7.92 | 9.73 | 12.62 | 17.26 |
| | | SDRL | 2.44 | 2.48 | 2.63 | 2.87 | 3.25 | 3.88 | 4.85 | 6.48 | 9.07 | 13.60 |
| | 2 | ARL | 4.81 | 4.81 | 4.88 | 4.98 | 5.23 | 5.66 | 6.41 | 7.74 | 10.11 | 14.82 |
| | | SDRL | 2.44 | 2.44 | 2.49 | 2.57 | 2.73 | 3.07 | 3.64 | 4.69 | 6.78 | 11.29 |
| | 3 | ARL | 4.80 | 4.82 | 4.82 | 4.86 | 4.98 | 5.21 | 5.70 | 6.64 | 8.57 | 12.95 |
| | | SDRL | 2.43 | 2.45 | 2.46 | 2.46 | 2.56 | 2.74 | 3.08 | 3.82 | 5.44 | 9.42 |
| 1.80 | 0 | ARL | 4.00 | 4.53 | 5.14 | 5.87 | 6.76 | 7.85 | 9.22 | 10.86 | 12.92 | 15.61 |
| | | SDRL | 1.91 | 2.25 | 2.67 | 3.21 | 3.90 | 4.79 | 6.01 | 7.48 | 9.42 | 12.03 |
| | 1 | ARL | 3.99 | 4.04 | 4.21 | 4.48 | 4.88 | 5.49 | 6.39 | 7.73 | 9.85 | 13.17 |
| | | SDRL | 1.90 | 1.93 | 2.05 | 2.22 | 2.49 | 2.93 | 3.60 | 4.71 | 6.56 | 9.61 |
| | 2 | ARL | 4.01 | 4.01 | 4.04 | 4.13 | 4.33 | 4.66 | 5.27 | 6.26 | 8.00 | 11.43 |
| | | SDRL | 1.91 | 1.92 | 1.94 | 1.99 | 2.11 | 2.35 | 2.76 | 3.51 | 4.95 | 7.99 |
| | 3 | ARL | 4.01 | 4.01 | 4.01 | 4.04 | 4.12 | 4.32 | 4.70 | 5.42 | 6.88 | 10.11 |
| | | SDRL | 1.91 | 1.92 | 1.92 | 1.93 | 1.98 | 2.11 | 2.37 | 2.88 | 4.01 | 6.84 |
| 2.00 | 0 | ARL | 3.42 | 3.85 | 4.36 | 4.94 | 5.64 | 6.49 | 7.51 | 8.76 | 10.34 | 12.25 |
| | | SDRL | 1.57 | 1.81 | 2.14 | 2.55 | 3.04 | 3.68 | 4.53 | 5.59 | 7.00 | 8.79 |
| | 1 | ARL | 3.42 | 3.45 | 3.59 | 3.80 | 4.14 | 4.64 | 5.33 | 6.39 | 7.99 | 10.50 |
| | | SDRL | 1.57 | 1.59 | 1.66 | 1.79 | 2.00 | 2.32 | 2.81 | 3.62 | 4.93 | 7.18 |
| | 2 | ARL | 3.42 | 3.43 | 3.44 | 3.53 | 3.68 | 3.97 | 4.44 | 5.23 | 6.60 | 9.20 |
| | | SDRL | 1.57 | 1.57 | 1.58 | 1.63 | 1.71 | 1.89 | 2.19 | 2.74 | 3.78 | 5.98 |
| | 3 | ARL | 3.42 | 3.43 | 3.42 | 3.45 | 3.53 | 3.67 | 3.98 | 4.58 | 5.71 | 8.16 |
| | | SDRL | 1.57 | 1.57 | 1.57 | 1.58 | 1.63 | 1.72 | 1.90 | 2.28 | 3.08 | 5.07 |

**TABLE 3.** Zero-state $ARL_1$ profile of the DCCUSUM chart with $ARL_0 = 500$.

| δ↓ | S↓ | ϕ→ | 0.0 | 0.1 | 0.2 | 0.3 | 0.4 | 0.5 | 0.6 | 0.7 | 0.8 | 0.9 |
|---|---|---|---|---|---|---|---|---|---|---|---|---|
| 0.20 | 0 | ARL | 270.28 | 290.70 | 310.03 | 329.77 | 347.27 | 366.48 | 378.72 | 396.26 | 408.01 | 421.21 |
| | | SDRL | 268.36 | 288.15 | 307.61 | 325.86 | 343.62 | 364.64 | 375.72 | 394.63 | 403.54 | 419.44 |
| | 1 | ARL | 268.61 | 271.33 | 277.70 | 286.40 | 302.40 | 317.80 | 340.86 | 363.79 | 384.35 | 410.06 |
| | | SDRL | 265.02 | 267.85 | 274.45 | 283.82 | 299.05 | 314.77 | 335.84 | 359.01 | 379.63 | 407.53 |
| | 2 | ARL | 268.36 | 270.46 | 271.69 | 275.08 | 280.90 | 296.12 | 313.29 | 338.31 | 367.77 | 400.24 |
| | | SDRL | 264.64 | 268.75 | 267.51 | 270.54 | 276.71 | 293.48 | 310.51 | 336.33 | 366.55 | 397.05 |
| | 3 | ARL | 268.32 | 266.98 | 269.96 | 271.13 | 273.82 | 283.03 | 297.58 | 317.51 | 349.12 | 391.08 |
| | | SDRL | 264.63 | 263.42 | 266.73 | 266.23 | 270.88 | 279.81 | 295.86 | 313.53 | 346.29 | 389.12 |
| 0.40 | 0 | ARL | 94.42 | 110.45 | 127.62 | 146.07 | 166.59 | 187.50 | 208.98 | 234.38 | 255.13 | 277.09 |
| | | SDRL | 90.59 | 106.79 | 124.28 | 142.10 | 162.75 | 184.38 | 205.23 | 231.25 | 251.36 | 273.43 |
| | 1 | ARL | 93.86 | 95.56 | 100.58 | 108.65 | 121.01 | 137.49 | 158.41 | 186.16 | 219.41 | 256.58 |
| | | SDRL | 89.40 | 91.50 | 96.83 | 104.05 | 116.51 | 133.52 | 154.43 | 182.94 | 215.48 | 252.12 |
| | 2 | ARL | 93.86 | 94.54 | 95.52 | 98.22 | 104.44 | 114.83 | 130.41 | 154.09 | 191.25 | 238.79 |
| | | SDRL | 89.70 | 90.22 | 91.83 | 94.33 | 100.48 | 111.09 | 126.03 | 150.03 | 187.51 | 234.52 |
| | 3 | ARL | 93.88 | 94.20 | 94.18 | 95.40 | 98.45 | 103.42 | 115.01 | 135.52 | 168.26 | 222.68 |
| | | SDRL | 89.86 | 89.99 | 89.36 | 91.05 | 94.11 | 99.51 | 110.81 | 132.19 | 164.90 | 219.14 |
| 0.60 | 0 | ARL | 38.06 | 45.79 | 55.12 | 66.09 | 78.91 | 92.84 | 108.80 | 127.09 | 147.06 | 167.13 |
| | | SDRL | 33.77 | 41.15 | 50.61 | 61.53 | 74.58 | 88.49 | 104.81 | 123.82 | 143.98 | 162.74 |
| | 1 | ARL | 37.88 | 38.66 | 40.82 | 44.93 | 51.32 | 60.19 | 73.35 | 91.44 | 116.70 | 148.10 |
| | | SDRL | 33.53 | 34.46 | 36.35 | 40.54 | 46.73 | 56.14 | 68.77 | 86.99 | 113.79 | 144.31 |
| | 2 | ARL | 38.03 | 37.89 | 38.42 | 39.78 | 42.65 | 48.07 | 56.88 | 71.56 | 94.91 | 132.48 |
| | | SDRL | 33.76 | 33.57 | 34.04 | 35.57 | 38.17 | 43.55 | 52.61 | 66.92 | 90.62 | 128.47 |
| | 3 | ARL | 37.83 | 37.86 | 38.12 | 38.48 | 39.78 | 42.61 | 48.27 | 59.38 | 79.72 | 118.04 |
| | | SDRL | 33.20 | 33.53 | 33.78 | 34.06 | 35.49 | 38.26 | 43.84 | 55.25 | 75.43 | 114.33 |
| 0.80 | 0 | ARL | 19.14 | 23.05 | 27.84 | 33.75 | 40.95 | 49.65 | 59.82 | 71.13 | 84.55 | 100.09 |
| | | SDRL | 14.95 | 18.71 | 23.44 | 29.36 | 36.67 | 45.10 | 55.50 | 66.69 | 80.20 | 96.00 |
| | 1 | ARL | 19.06 | 19.50 | 20.66 | 22.53 | 25.93 | 30.70 | 37.84 | 48.78 | 64.39 | 86.38 |
| | | SDRL | 14.84 | 15.38 | 16.33 | 18.21 | 21.49 | 26.22 | 33.52 | 44.28 | 60.00 | 81.93 |
| | 2 | ARL | 19.07 | 19.20 | 19.38 | 20.11 | 21.57 | 24.11 | 28.69 | 36.64 | 50.47 | 75.01 |
| | | SDRL | 14.86 | 14.87 | 15.14 | 15.82 | 17.38 | 19.83 | 24.32 | 32.30 | 46.18 | 70.88 |
| | 3 | ARL | 19.09 | 19.07 | 19.11 | 19.42 | 20.02 | 21.43 | 24.29 | 29.91 | 41.60 | 65.81 |
| | | SDRL | 14.92 | 14.90 | 14.92 | 15.27 | 15.85 | 17.19 | 20.00 | 25.64 | 37.30 | 61.41 |
| 1.00 | 0 | ARL | 11.66 | 13.80 | 16.45 | 19.86 | 23.94 | 29.09 | 35.16 | 42.78 | 51.85 | 62.22 |
| | | SDRL | 7.91 | 9.88 | 12.30 | 15.68 | 19.55 | 24.76 | 31.03 | 38.50 | 47.60 | 57.82 |
| | 1 | ARL | 11.66 | 11.91 | 12.48 | 13.60 | 15.38 | 18.14 | 22.17 | 28.61 | 38.22 | 52.63 |
| | | SDRL | 7.84 | 8.09 | 8.66 | 9.67 | 11.37 | 13.99 | 17.91 | 24.34 | 33.79 | 48.33 |
| | 2 | ARL | 11.67 | 11.70 | 11.83 | 12.19 | 13.01 | 14.47 | 16.94 | 21.52 | 29.72 | 45.30 |
| | | SDRL | 7.88 | 7.93 | 8.03 | 8.40 | 9.14 | 10.45 | 12.85 | 17.22 | 25.29 | 40.94 |
| | 3 | ARL | 11.72 | 11.63 | 11.69 | 11.83 | 12.18 | 12.93 | 14.52 | 17.72 | 24.40 | 39.38 |
| | | SDRL | 7.93 | 7.86 | 7.87 | 7.99 | 8.34 | 9.01 | 10.59 | 13.63 | 20.18 | 35.18 |
| 1.20 | 0 | ARL | 8.15 | 9.46 | 11.10 | 13.21 | 15.66 | 18.83 | 22.71 | 27.60 | 33.57 | 40.82 |
| | | SDRL | 4.82 | 5.93 | 7.37 | 9.33 | 11.67 | 14.64 | 18.40 | 23.21 | 29.27 | 36.45 |
| | 1 | ARL | 8.12 | 8.26 | 8.63 | 9.33 | 10.37 | 12.11 | 14.60 | 18.54 | 24.59 | 34.28 |
| | | SDRL | 4.81 | 4.92 | 5.23 | 5.82 | 6.72 | 8.33 | 10.60 | 14.36 | 20.31 | 29.90 |
| | 2 | ARL | 8.10 | 8.13 | 8.24 | 8.46 | 8.97 | 9.87 | 11.43 | 14.18 | 19.33 | 29.22 |
| | | SDRL | 4.79 | 4.80 | 4.91 | 5.06 | 5.49 | 6.29 | 7.68 | 10.23 | 15.13 | 24.83 |
| | 3 | ARL | 8.15 | 8.14 | 8.14 | 8.25 | 8.45 | 8.94 | 9.92 | 11.89 | 15.94 | 25.39 |
| | | SDRL | 4.82 | 4.77 | 4.81 | 4.89 | 5.08 | 5.48 | 6.32 | 8.07 | 11.89 | 21.08 |
| 1.40 | 0 | ARL | 6.17 | 7.11 | 8.19 | 9.56 | 11.25 | 13.34 | 16.01 | 19.23 | 23.35 | 28.21 |
| | | SDRL | 3.27 | 3.99 | 4.87 | 6.04 | 7.51 | 9.46 | 11.96 | 15.09 | 19.11 | 23.86 |
| | 1 | ARL | 6.19 | 6.26 | 6.52 | 7.01 | 7.75 | 8.86 | 10.57 | 13.15 | 17.11 | 23.73 |
| | | SDRL | 3.28 | 3.33 | 3.53 | 3.91 | 4.46 | 5.41 | 6.91 | 9.24 | 13.05 | 19.53 |
| | 2 | ARL | 6.17 | 6.17 | 6.23 | 6.39 | 6.75 | 7.36 | 8.39 | 10.27 | 13.63 | 20.33 |
| | | SDRL | 3.26 | 3.27 | 3.29 | 3.46 | 3.72 | 4.17 | 5.03 | 6.65 | 9.66 | 16.19 |
| | 3 | ARL | 6.16 | 6.15 | 6.17 | 6.23 | 6.38 | 6.73 | 7.42 | 8.71 | 11.45 | 17.72 |

**TABLE 3.** ***(Continued.)*** **Zero-state $ARL_1$ profile of the DCCUSUM chart with $ARL_0 = 500$.**

| | | | | | | | | | | | | |
|---|---|---|---|---|---|---|---|---|---|---|---|---|
| | | SDRL | 3.26 | 3.25 | 3.27 | 3.32 | 3.41 | 3.68 | 4.23 | 5.28 | 7.68 | 13.55 |
| 1.60 | 0 | ARL | 4.95 | 5.65 | 6.45 | 7.43 | 8.67 | 10.11 | 11.91 | 14.20 | 16.98 | 20.50 |
| | | SDRL | 2.41 | 2.90 | 3.48 | 4.25 | 5.28 | 6.48 | 8.12 | 10.25 | 12.81 | 16.29 |
| | 1 | ARL | 4.95 | 5.00 | 5.21 | 5.55 | 6.11 | 6.91 | 8.11 | 9.89 | 12.78 | 17.36 |
| | | SDRL | 2.41 | 2.44 | 2.57 | 2.83 | 3.21 | 3.85 | 4.79 | 6.30 | 8.91 | 13.27 |
| | 2 | ARL | 4.93 | 4.96 | 5.00 | 5.12 | 5.38 | 5.82 | 6.58 | 7.90 | 10.30 | 14.99 |
| | | SDRL | 2.40 | 2.41 | 2.44 | 2.52 | 2.69 | 3.01 | 3.57 | 4.64 | 6.69 | 10.98 |
| | 3 | ARL | 4.95 | 4.94 | 4.94 | 4.99 | 5.11 | 5.37 | 5.86 | 6.82 | 8.77 | 13.16 |
| | | SDRL | 2.42 | 2.40 | 2.40 | 2.42 | 2.52 | 2.70 | 3.04 | 3.76 | 5.35 | 9.26 |
| 1.80 | 0 | ARL | 4.12 | 4.66 | 5.28 | 6.03 | 6.92 | 8.05 | 9.37 | 11.05 | 13.12 | 15.71 |
| | | SDRL | 1.88 | 2.23 | 2.65 | 3.15 | 3.84 | 4.75 | 5.83 | 7.31 | 9.19 | 11.68 |
| | 1 | ARL | 4.12 | 4.18 | 4.33 | 4.60 | 5.02 | 5.64 | 6.56 | 7.91 | 10.01 | 13.36 |
| | | SDRL | 1.88 | 1.93 | 2.02 | 2.19 | 2.45 | 2.89 | 3.57 | 4.63 | 6.43 | 9.40 |
| | 2 | ARL | 4.12 | 4.13 | 4.17 | 4.25 | 4.45 | 4.81 | 5.41 | 6.41 | 8.19 | 11.56 |
| | | SDRL | 1.88 | 1.90 | 1.92 | 1.97 | 2.10 | 2.31 | 2.71 | 3.44 | 4.85 | 7.78 |
| | 3 | ARL | 4.12 | 4.11 | 4.12 | 4.16 | 4.23 | 4.46 | 4.84 | 5.58 | 7.04 | 10.30 |
| | | SDRL | 1.89 | 1.89 | 1.89 | 1.91 | 1.96 | 2.08 | 2.34 | 2.86 | 3.92 | 6.67 |
| 2.00 | 0 | ARL | 3.52 | 3.96 | 4.47 | 5.08 | 5.80 | 6.63 | 7.68 | 8.99 | 10.53 | 12.46 |
| | | SDRL | 1.55 | 1.80 | 2.10 | 2.49 | 3.00 | 3.59 | 4.43 | 5.52 | 6.86 | 8.60 |
| | 1 | ARL | 3.52 | 3.56 | 3.69 | 3.92 | 4.26 | 4.77 | 5.48 | 6.58 | 8.18 | 10.72 |
| | | SDRL | 1.56 | 1.57 | 1.65 | 1.77 | 1.97 | 2.29 | 2.78 | 3.58 | 4.83 | 7.09 |
| | 2 | ARL | 3.53 | 3.53 | 3.55 | 3.63 | 3.80 | 4.09 | 4.56 | 5.37 | 6.75 | 9.40 |
| | | SDRL | 1.56 | 1.56 | 1.58 | 1.61 | 1.72 | 1.87 | 2.17 | 2.69 | 3.70 | 5.91 |
| | 3 | ARL | 3.52 | 3.52 | 3.53 | 3.56 | 3.62 | 3.79 | 4.12 | 4.71 | 5.87 | 8.37 |
| | | SDRL | 1.55 | 1.56 | 1.56 | 1.57 | 1.61 | 1.70 | 1.89 | 2.26 | 3.05 | 5.02 |

**TABLE 4.** **Steady-state $ARL_1$ profile of the DCCUSUM with $ARL_0 = 500$.**

| δ↓ | S↓ | ϕ→ | 0.0 | 0.1 | 0.2 | 0.3 | 0.4 | 0.5 | 0.6 | 0.7 | 0.8 | 0.9 |
|---|---|---|---|---|---|---|---|---|---|---|---|---|
| 0.20 | 0 | ARL | 269.30 | 290.34 | 309.98 | 329.02 | 350.83 | 364.68 | 383.27 | 395.61 | 410.30 | 422.40 |
| | | SDRL | 267.60 | 287.61 | 308.70 | 327.63 | 348.77 | 365.01 | 383.68 | 394.07 | 409.05 | 421.11 |
| | 1 | ARL | 268.99 | 271.21 | 277.42 | 285.97 | 304.08 | 320.18 | 340.71 | 367.43 | 387.21 | 408.27 |
| | | SDRL | 267.51 | 269.30 | 276.64 | 284.58 | 303.63 | 320.51 | 341.61 | 363.95 | 386.92 | 407.02 |
| | 2 | ARL | 270.23 | 269.52 | 271.67 | 274.97 | 282.89 | 295.55 | 314.60 | 338.77 | 368.16 | 397.68 |
| | | SDRL | 268.02 | 267.19 | 270.61 | 274.22 | 281.49 | 293.78 | 312.27 | 337.82 | 368.71 | 397.36 |
| | 3 | ARL | 269.19 | 267.57 | 269.12 | 270.78 | 273.26 | 280.53 | 294.92 | 317.40 | 350.08 | 390.56 |
| | | SDRL | 266.82 | 266.47 | 267.65 | 269.23 | 272.93 | 279.18 | 293.59 | 316.20 | 349.89 | 388.21 |
| 0.40 | 0 | ARL | 93.71 | 110.20 | 128.10 | 146.18 | 166.49 | 186.41 | 209.33 | 232.86 | 254.85 | 276.28 |
| | | SDRL | 90.93 | 106.87 | 124.70 | 143.60 | 164.36 | 184.39 | 206.77 | 232.35 | 253.83 | 274.59 |
| | 1 | ARL | 93.92 | 95.37 | 99.87 | 108.03 | 120.18 | 135.97 | 157.61 | 185.75 | 218.72 | 256.13 |
| | | SDRL | 90.75 | 92.18 | 96.78 | 104.72 | 117.56 | 133.61 | 155.29 | 182.22 | 218.33 | 254.10 |
| | 2 | ARL | 93.77 | 93.73 | 95.11 | 97.98 | 103.48 | 114.11 | 130.18 | 155.03 | 191.48 | 238.84 |
| | | SDRL | 90.73 | 90.57 | 92.08 | 94.93 | 99.86 | 111.85 | 127.28 | 152.31 | 189.54 | 236.40 |
| | 3 | ARL | 93.90 | 94.14 | 94.23 | 94.78 | 97.50 | 103.18 | 114.98 | 134.45 | 169.25 | 223.84 |
| | | SDRL | 90.31 | 91.16 | 90.53 | 92.27 | 94.39 | 100.32 | 111.86 | 131.66 | 166.63 | 223.01 |
| 0.60 | 0 | ARL | 37.49 | 45.48 | 54.88 | 65.59 | 77.82 | 92.63 | 108.85 | 126.33 | 145.96 | 166.58 |
| | | SDRL | 33.62 | 41.75 | 51.24 | 62.04 | 74.80 | 89.45 | 105.52 | 123.40 | 143.82 | 163.80 |
| | 1 | ARL | 37.45 | 38.33 | 40.60 | 44.44 | 50.77 | 59.89 | 72.42 | 91.22 | 115.34 | 148.19 |
| | | SDRL | 33.73 | 34.76 | 36.76 | 40.62 | 47.08 | 56.17 | 69.32 | 87.48 | 112.08 | 146.13 |
| | 2 | ARL | 37.30 | 37.65 | 38.04 | 39.47 | 42.65 | 47.48 | 56.09 | 70.73 | 94.87 | 132.70 |
| | | SDRL | 33.43 | 33.86 | 34.32 | 35.46 | 38.91 | 43.73 | 52.64 | 67.32 | 91.23 | 129.28 |
| | 3 | ARL | 37.53 | 37.68 | 37.72 | 38.07 | 39.51 | 42.42 | 48.08 | 58.98 | 79.47 | 118.17 |
| | | SDRL | 33.68 | 33.84 | 33.81 | 34.21 | 35.62 | 38.71 | 44.58 | 55.20 | 75.93 | 114.36 |

**TABLE 4.** ***(Continued.)*** **Steady-state $ARL_1$ profile of the DCCUSUM with $ARL_0 = 500$.**

| | | | | | | | | | | | | |
|---|---|---|---|---|---|---|---|---|---|---|---|---|
| 0.80 | 0 | ARL | 18.81 | 22.71 | 27.48 | 33.26 | 40.44 | 49.28 | 58.96 | 70.58 | 84.36 | 99.83 |
| | | SDRL | 14.98 | 18.91 | 23.55 | 29.33 | 36.75 | 45.74 | 55.31 | 67.09 | 81.26 | 96.88 |
| | 1 | ARL | 18.86 | 19.21 | 20.32 | 22.28 | 25.50 | 30.11 | 37.68 | 47.84 | 63.94 | 86.12 |
| | | SDRL | 15.05 | 15.36 | 16.47 | 18.36 | 21.62 | 26.28 | 33.72 | 44.08 | 60.18 | 83.36 |
| | 2 | ARL | 18.80 | 18.81 | 19.11 | 19.79 | 21.34 | 23.86 | 28.38 | 36.04 | 50.12 | 74.58 |
| | | SDRL | 14.92 | 15.10 | 15.24 | 15.94 | 17.46 | 20.05 | 24.47 | 32.21 | 46.47 | 70.96 |
| | 3 | ARL | 18.81 | 18.81 | 18.86 | 19.09 | 19.77 | 21.23 | 23.86 | 29.75 | 41.09 | 65.45 |
| | | SDRL | 14.98 | 14.95 | 15.01 | 15.30 | 15.87 | 17.21 | 20.00 | 25.82 | 37.40 | 61.79 |
| 1.00 | 0 | ARL | 11.49 | 13.63 | 16.30 | 19.49 | 23.61 | 28.61 | 35.00 | 42.37 | 51.23 | 62.05 |
| | | SDRL | 7.94 | 9.97 | 12.52 | 15.68 | 19.80 | 24.74 | 31.27 | 38.36 | 47.75 | 58.29 |
| | 1 | ARL | 11.45 | 11.69 | 12.25 | 13.33 | 15.14 | 17.83 | 21.87 | 27.88 | 37.72 | 52.52 |
| | | SDRL | 7.91 | 8.20 | 8.72 | 9.63 | 11.36 | 14.03 | 17.97 | 23.90 | 33.98 | 49.16 |
| | 2 | ARL | 11.45 | 11.47 | 11.64 | 12.00 | 12.76 | 14.18 | 16.71 | 21.19 | 29.34 | 45.03 |
| | | SDRL | 7.98 | 8.00 | 8.09 | 8.45 | 9.17 | 10.52 | 12.84 | 17.36 | 25.72 | 41.29 |
| | 3 | ARL | 11.45 | 11.49 | 11.46 | 11.64 | 11.94 | 12.74 | 14.32 | 17.50 | 24.16 | 39.10 |
| | | SDRL | 7.91 | 7.95 | 7.96 | 8.11 | 8.37 | 9.11 | 10.62 | 13.72 | 20.35 | 35.35 |
| 1.20 | 0 | ARL | 7.98 | 9.32 | 10.94 | 12.94 | 15.44 | 18.69 | 22.50 | 27.34 | 33.29 | 40.42 |
| | | SDRL | 4.85 | 6.01 | 7.49 | 9.32 | 11.65 | 14.85 | 18.66 | 23.39 | 29.53 | 36.54 |
| | 1 | ARL | 7.97 | 8.08 | 8.49 | 9.15 | 10.22 | 11.85 | 14.38 | 18.27 | 24.32 | 33.92 |
| | | SDRL | 4.87 | 4.93 | 5.30 | 5.90 | 6.83 | 8.31 | 10.64 | 14.49 | 20.50 | 30.01 |
| | 2 | ARL | 7.98 | 7.99 | 8.08 | 8.32 | 8.80 | 9.65 | 11.22 | 13.94 | 19.00 | 28.98 |
| | | SDRL | 4.85 | 4.87 | 4.93 | 5.17 | 5.57 | 6.30 | 7.72 | 10.28 | 15.12 | 25.01 |
| | 3 | ARL | 7.97 | 8.01 | 8.03 | 8.08 | 8.32 | 8.78 | 9.77 | 11.70 | 15.69 | 24.95 |
| | | SDRL | 4.86 | 4.88 | 4.88 | 4.95 | 5.13 | 5.53 | 6.38 | 8.14 | 11.95 | 21.02 |
| 1.40 | 0 | ARL | 6.06 | 6.95 | 8.08 | 9.41 | 11.06 | 13.17 | 15.68 | 18.94 | 22.89 | 28.01 |
| | | SDRL | 3.34 | 4.04 | 4.94 | 6.05 | 7.59 | 9.51 | 11.90 | 15.19 | 19.09 | 24.01 |
| | 1 | ARL | 6.06 | 6.14 | 6.39 | 6.87 | 7.60 | 8.70 | 10.34 | 12.94 | 16.93 | 23.28 |
| | | SDRL | 3.32 | 3.38 | 3.58 | 3.95 | 4.53 | 5.46 | 6.92 | 9.29 | 13.15 | 19.44 |
| | 2 | ARL | 6.05 | 6.05 | 6.15 | 6.30 | 6.62 | 7.20 | 8.25 | 10.02 | 13.40 | 20.12 |
| | | SDRL | 3.31 | 3.33 | 3.39 | 3.51 | 3.76 | 4.23 | 5.06 | 6.60 | 9.74 | 16.25 |
| | 3 | ARL | 6.07 | 6.05 | 6.09 | 6.12 | 6.27 | 6.62 | 7.28 | 8.58 | 11.24 | 17.46 |
| | | SDRL | 3.32 | 3.30 | 3.34 | 3.36 | 3.49 | 3.76 | 4.29 | 5.36 | 7.69 | 13.55 |
| 1.60 | 0 | ARL | 4.87 | 5.53 | 6.34 | 7.31 | 8.47 | 9.92 | 11.76 | 13.97 | 16.74 | 20.14 |
| | | SDRL | 2.46 | 2.93 | 3.54 | 4.30 | 5.27 | 6.51 | 8.22 | 10.31 | 12.95 | 16.21 |
| | 1 | ARL | 4.87 | 4.92 | 5.12 | 5.48 | 6.01 | 6.80 | 7.98 | 9.75 | 12.55 | 17.13 |
| | | SDRL | 2.47 | 2.50 | 2.62 | 2.89 | 3.28 | 3.88 | 4.85 | 6.40 | 8.92 | 13.35 |
| | 2 | ARL | 4.87 | 4.87 | 4.91 | 5.04 | 5.28 | 5.74 | 6.48 | 7.77 | 10.09 | 14.66 |
| | | SDRL | 2.47 | 2.47 | 2.49 | 2.59 | 2.74 | 3.09 | 3.64 | 4.70 | 6.69 | 10.94 |
| | 3 | ARL | 4.86 | 4.86 | 4.88 | 4.92 | 5.03 | 5.26 | 5.76 | 6.69 | 8.56 | 12.94 |
| | | SDRL | 2.46 | 2.46 | 2.47 | 2.51 | 2.59 | 2.76 | 3.08 | 3.80 | 5.38 | 9.30 |
| 1.80 | 0 | ARL | 4.04 | 4.58 | 5.21 | 5.93 | 6.82 | 7.92 | 9.26 | 10.87 | 12.87 | 15.40 |
| | | SDRL | 1.94 | 2.28 | 2.68 | 3.21 | 3.93 | 4.82 | 5.95 | 7.41 | 9.27 | 11.66 |
| | 1 | ARL | 4.05 | 4.10 | 4.26 | 4.52 | 4.94 | 5.56 | 6.45 | 7.79 | 9.85 | 13.14 |
| | | SDRL | 1.95 | 1.97 | 2.07 | 2.25 | 2.51 | 2.94 | 3.63 | 4.73 | 6.52 | 9.50 |
| | 2 | ARL | 4.04 | 4.06 | 4.10 | 4.19 | 4.38 | 4.73 | 5.30 | 6.29 | 8.03 | 11.42 |
| | | SDRL | 1.94 | 1.95 | 1.97 | 2.03 | 2.16 | 2.39 | 2.78 | 3.52 | 4.90 | 7.92 |
| | 3 | ARL | 4.05 | 4.04 | 4.06 | 4.09 | 4.18 | 4.38 | 4.75 | 5.48 | 6.89 | 10.09 |
| | | SDRL | 1.95 | 1.95 | 1.96 | 1.99 | 2.03 | 2.16 | 2.39 | 2.90 | 3.97 | 6.72 |
| 2.00 | 0 | ARL | 3.46 | 3.91 | 4.40 | 4.98 | 5.70 | 6.51 | 7.55 | 8.81 | 10.29 | 12.23 |
| | | SDRL | 1.61 | 1.86 | 2.16 | 2.55 | 3.05 | 3.65 | 4.50 | 5.55 | 6.85 | 8.63 |
| | 1 | ARL | 3.45 | 3.49 | 3.61 | 3.85 | 4.19 | 4.69 | 5.40 | 6.44 | 8.01 | 10.51 |
| | | SDRL | 1.60 | 1.63 | 1.70 | 1.83 | 2.04 | 2.35 | 2.83 | 3.63 | 4.90 | 7.04 |
| | 2 | ARL | 3.47 | 3.47 | 3.49 | 3.58 | 3.73 | 4.02 | 4.47 | 5.28 | 6.65 | 9.23 |
| | | SDRL | 1.62 | 1.62 | 1.63 | 1.67 | 1.76 | 1.93 | 2.21 | 2.75 | 3.76 | 5.94 |
| | 3 | ARL | 3.46 | 3.46 | 3.47 | 3.49 | 3.57 | 3.72 | 4.05 | 4.63 | 5.76 | 8.23 |
| | | SDRL | 1.61 | 1.61 | 1.62 | 1.61 | 1.67 | 1.76 | 1.94 | 2.31 | 3.10 | 5.07 |

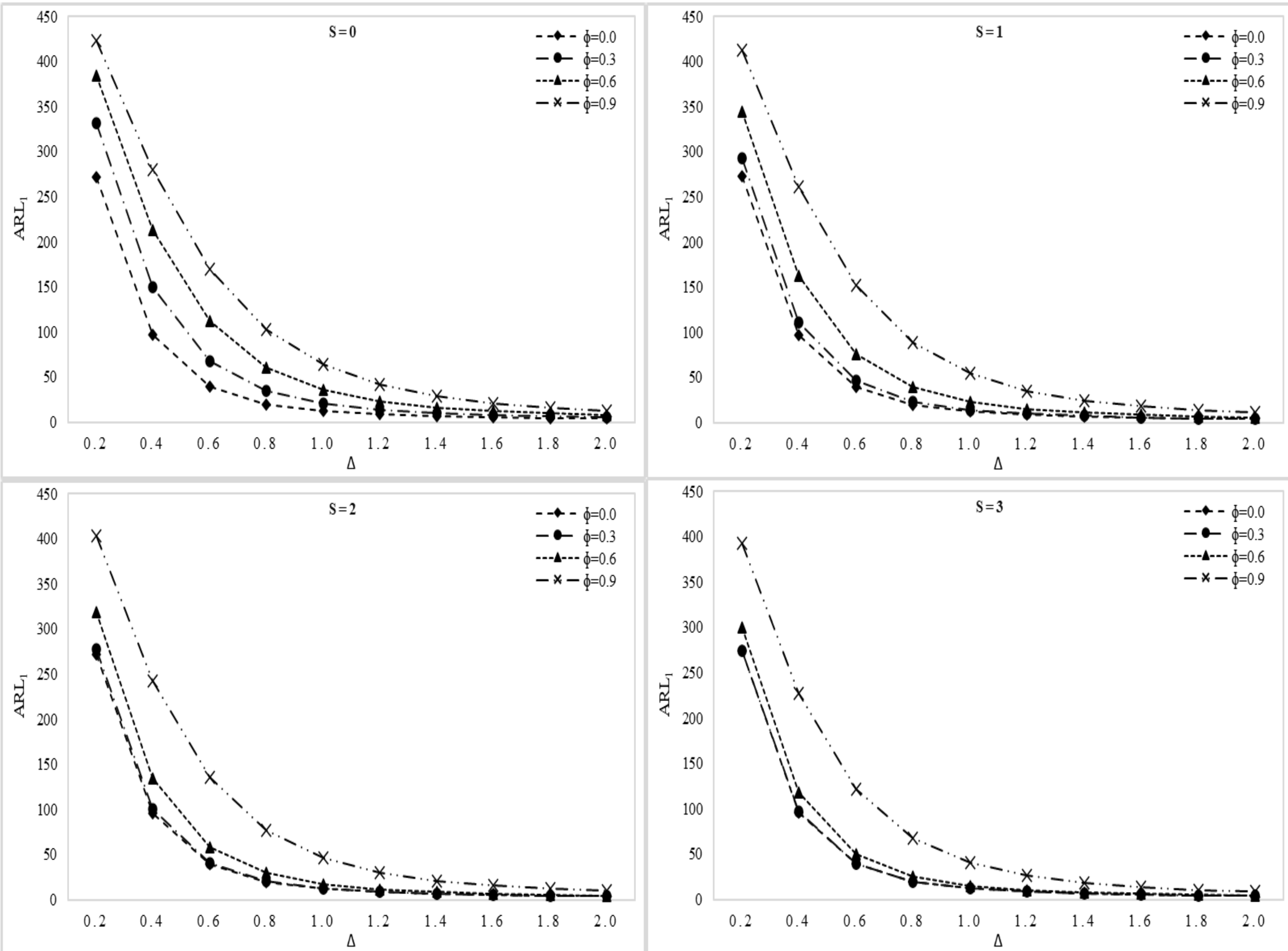


**FIGURE 1.** **Zero-state ARL Curves for DCUSUM chart at s = 0, s = 1, s = 2 and s = 3.**

quite similar to that of the CUSUM, but the former provides slightly better performance. To improve the CUSUM and EWMA charts' sensitivity to large shifts and to detect simultaneously both small and large size shifts through a single chart, Lucas [6] integrated the Shewhart chart with the CUSUM and Klein [7] combined the Shewhart with EWMA and suggested the combined Shewhart-CUSUM and combined Shewhart-EWMA charts, respectively. The fast initial response (FIR)-based CUSUM, referred to as the FIR-CUSUM chart, was proposed by Lucas and Crosier [8] by combining the CUSUM chart with a head-start feature. The FIR-CUSUM chart detects mean shifts in the early/start-up process faster than the CUSUM chart. Steiner [9] proposed incorporating a FIR feature into the EWMA chart. The said charts, as well as their extensions and mixed versions, are well documented in the literature in order to improve the detection speed when signaling a change in an ongoing process parameter (s).

Actually, it is difficult to predetermine the exact size of the shifts in most practical process monitoring. Therefore, a more suitable choice is to detect a range of shifts based on prior engineering knowledge and information from historical data, instead of the pre-assumed shift size. While traditional EWMA and CUSUM CCs are not intended to monitor a wide range of process shifts, Failure to accommodate a range of mean-shift values may reduce a system's ability to trigger corrected signals. To overcome this issue, Zhao et al. [10] first proposed a dual CUSUM (DCUSUM) chart for monitoring a variety of process mean shifts. The DCUSUM chart is more sensitive than the CUSUM and the Shewhart-CUSUM charts. Similarly, Haq and Lubna [11] proposed a new dual CCUSUM chart, referred to as DCCUSUM, which provides greater sensitivity than the DCUSUM chart. These charts are a combination of two separate CUSUM/CCUSUM charts, one of which is sensitive to small to moderate size shifts and the other to moderate to large size shifts. In the SPC literature, the DCUSUM and DCCUSUM CCs have received considerable attention because of their excellent detection abilities in detecting a range of process mean shifts. Recent publications on dual CUSUM charts include (cf., [12] and [16]), and many others.

Autocorrelation is a common practice in many processes, which could be due to the fundamental process dynamics. Furthermore, as measurement and data collection

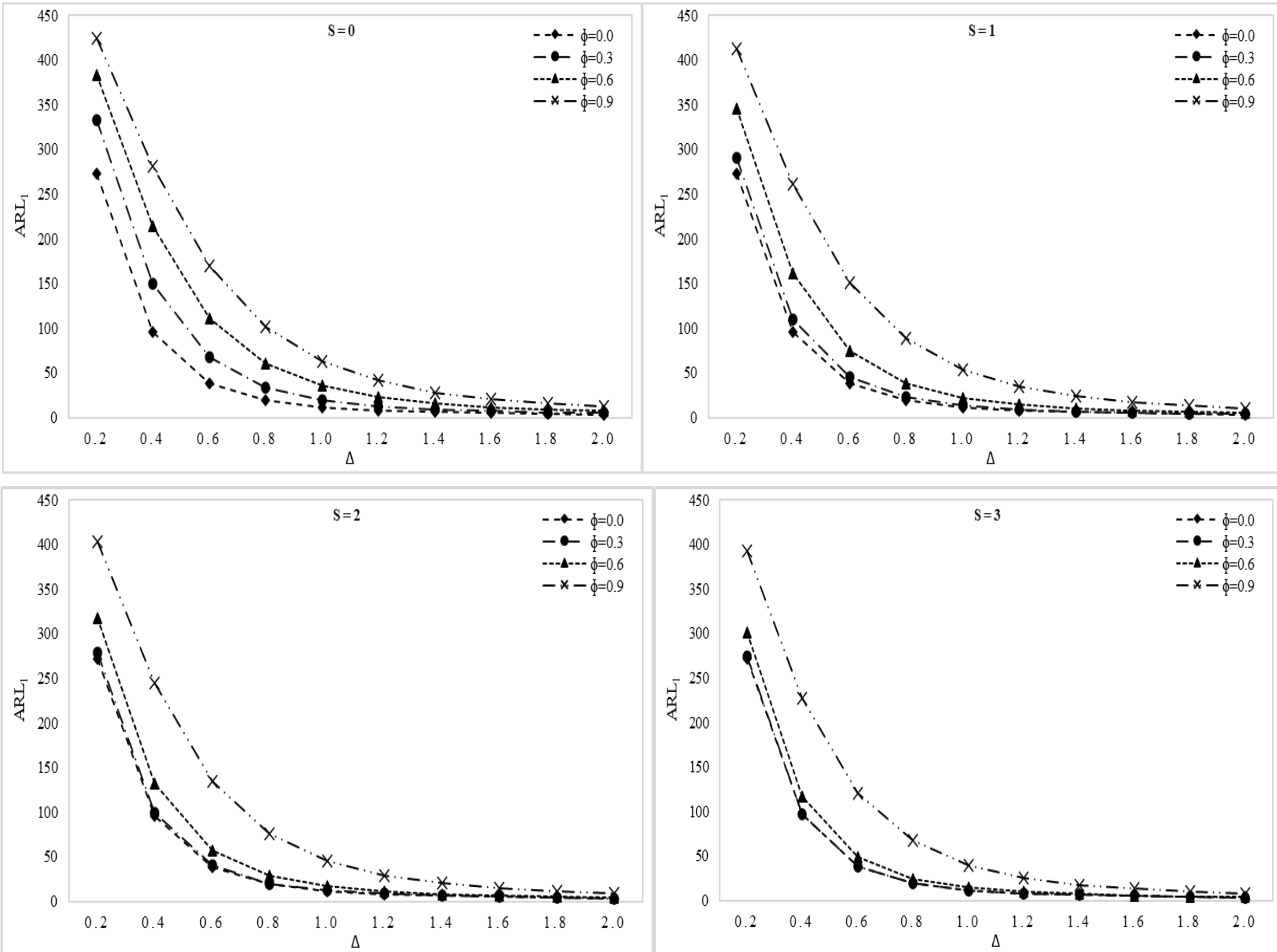


**FIGURE 2.** Steady-state ARL Curves for DCUSUM chart at s = 0, s = 1, s = 2 and s = 3.

technologies have become more automated in recent years, a process can now be sampled at higher frequencies, resulting in autocorrelation. Consequently, when there is autocorrelation in data, it might have a significant negative impact on a CC's performance. Positive autocorrelation, for example, can cause substantial negative bias in classical estimators of the process standard deviation, resulting in considerably tighter control limits than anticipated. When tight control limitations are paired with autocorrelation in the plotted observations, the average false alarm rate can be significantly greater than the expected one. Because of the high probability of false alarms, the process staff has to waste much time looking for unusual causes. This can lead to a loss of trust in the CC, and possibly the termination of the process monitoring. As a result, autocorrelation should not be overlooked when creating CCs, because failure to correctly account for autocorrelation can significantly reduce or eliminate a CC's effectiveness. Recently, Costa and Castagliola [17] investigated the performance of the Shewhart $\bar{X}$ control chart under the separated and combined effects of autocorrelation and measurement errors when the observations can be modelled as an AR(1) model and they proposed the idea of building up the samples with the non-neighboring items, such as from the production line, and s-skipping one, two, or more before selecting the next. Many researchers have developed the control charts for monitoring the autocorrelated process parameter in a variety of scenarios, see for instance, (cf., [18] and [25]), a few cited therein.

The research on the DCUSUM and DCCUSUM CCs are studied under the assumption that observations follow iid. However, in practice, the observed process measurements are collected automatically at high sampling rates, and their consecutive values are serially correlated, with the following consequences: i) invalidating the iid assumption, ii) inability to identify variation caused by random/special causes, iii) increasing false alarms, and iv) compromising the effectiveness of the charts for fault detection, and so on, for more details, refer to (cf., [26] and [32]), a few cited therein. In this article we propose the DCUSUM and DCCUSUM charts for monitoring the mean of the autocorrelated processes and

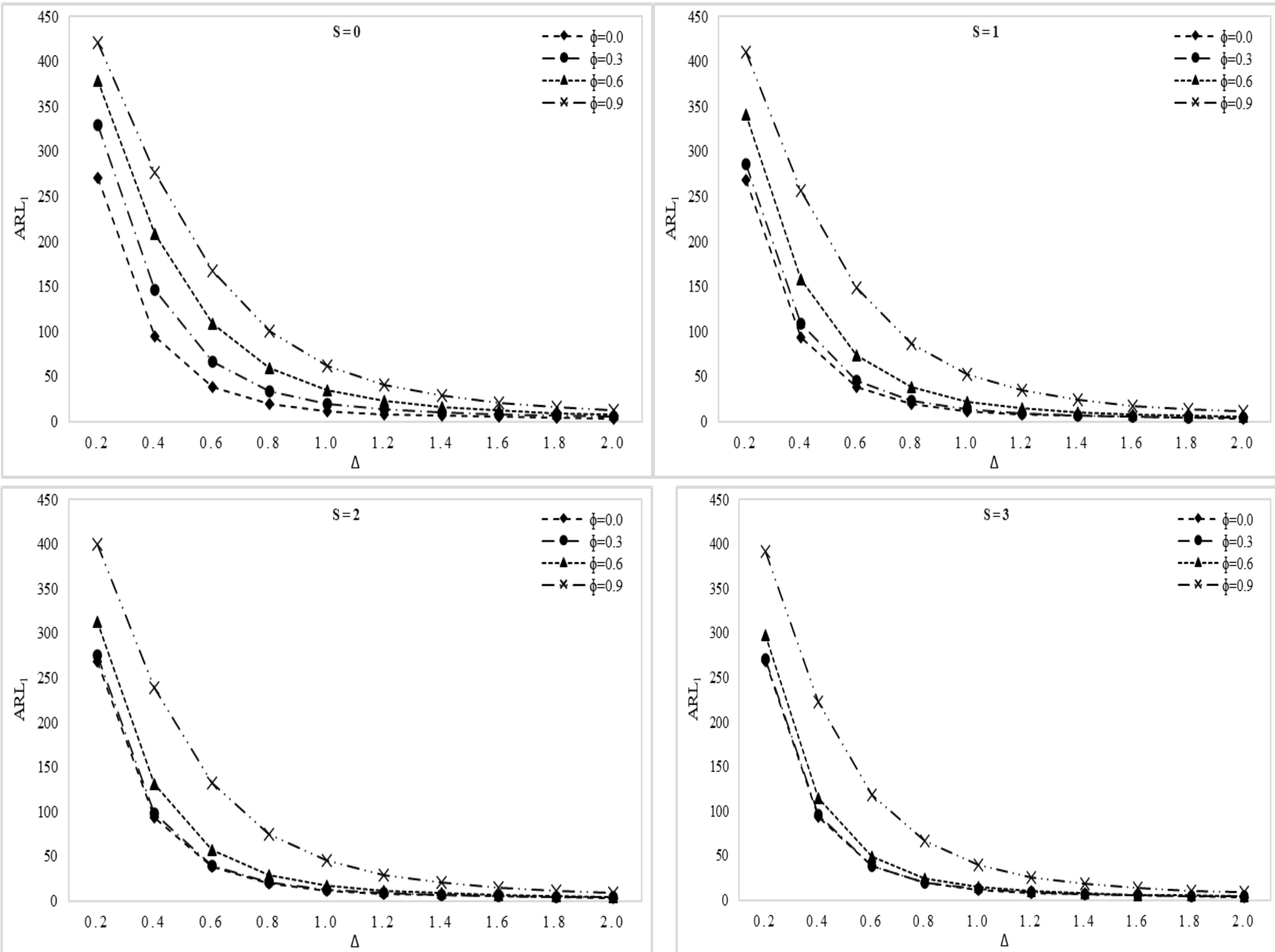


**FIGURE 3.** Zero-state ARL Curves for DCCUSUM chart at s = 0, s = 1, s = 2 and s = 3.

employs the s-skipping sampling strategy as a remedy to counter the adverse effect of autocorrelation. The run length's average and standard deviation (abbreviated as ARL and SDRL, respectively) and some overall performance comparison measures, such as the extra quadratic loss (EQL), relative average run length (RARL), and performance comparison index (PCI), are obtained using the Monte-Carlo simulation algorithm to evaluate the CC's performance.

The remaining paper is organized as follows: The structure of the DCUSUM and DCCUSUM, as well as the models for the autocorrelation effect, are discussed in Section 2. Section 3 investigates the effect of autocorrelation on both charts; Section 4 offers a simulation-based comparative analysis; and Section 5 offers a simulated data-based implementation example. Finally, Section 6 concludes with recommendations.

## II. A REVIEW OF THE TWO DUAL CUSUM CHARTS

This section provides a brief overview of dual CUSUM charts for monitoring the range of process mean shifts when the observations are assumed to be independently identically normally distributed (i.i.d).

Let $\{X_{t,i}; t \geq 1; i = 1, 2, \ldots, n\}$ represent under-consideration observations of the quality characteristic, and assume $X_{t,i}$ has a normal distribution with parameters: mean $\mu$ and variance $\sigma^2$ at $t$ time, ie, $X_{t,i} \sim N(\mu, \sigma^2)$ for $t \geq 1$. To monitor changes in the mean parameter, a sample of size $n : (X_{t,1}, X_{t,2}, \ldots, X_{t,n})$, is repeatedly taken from the process at time $t$, then $\bar{X}_t = \frac{1}{n}\sum_{i=1}^{n} X_{t,i}$, is computed. Assume that a process $\{X_{t,i}\}$ is in the IC state up until a certain time point (let's say $t \leq t_0$) and then goes OC due to the occurrence of an unknown shift $\delta$ in the process mean $\mu$, leading to $X_t \sim N(\mu_1, \sigma^2)$ when $t > t_0$. Here $\delta$ is the standardised shift: $|\mu_1 - \mu_0|/(\sigma n^{-0.5})$ and $\mu_0$ is the IC process mean.

### A. THE DCUSUM CHART

In practice, the shift size is frequently unknown, whereas the CUSUM charts' performance is based only on a given size of shift. As a result, traditional CUSUM charts may not

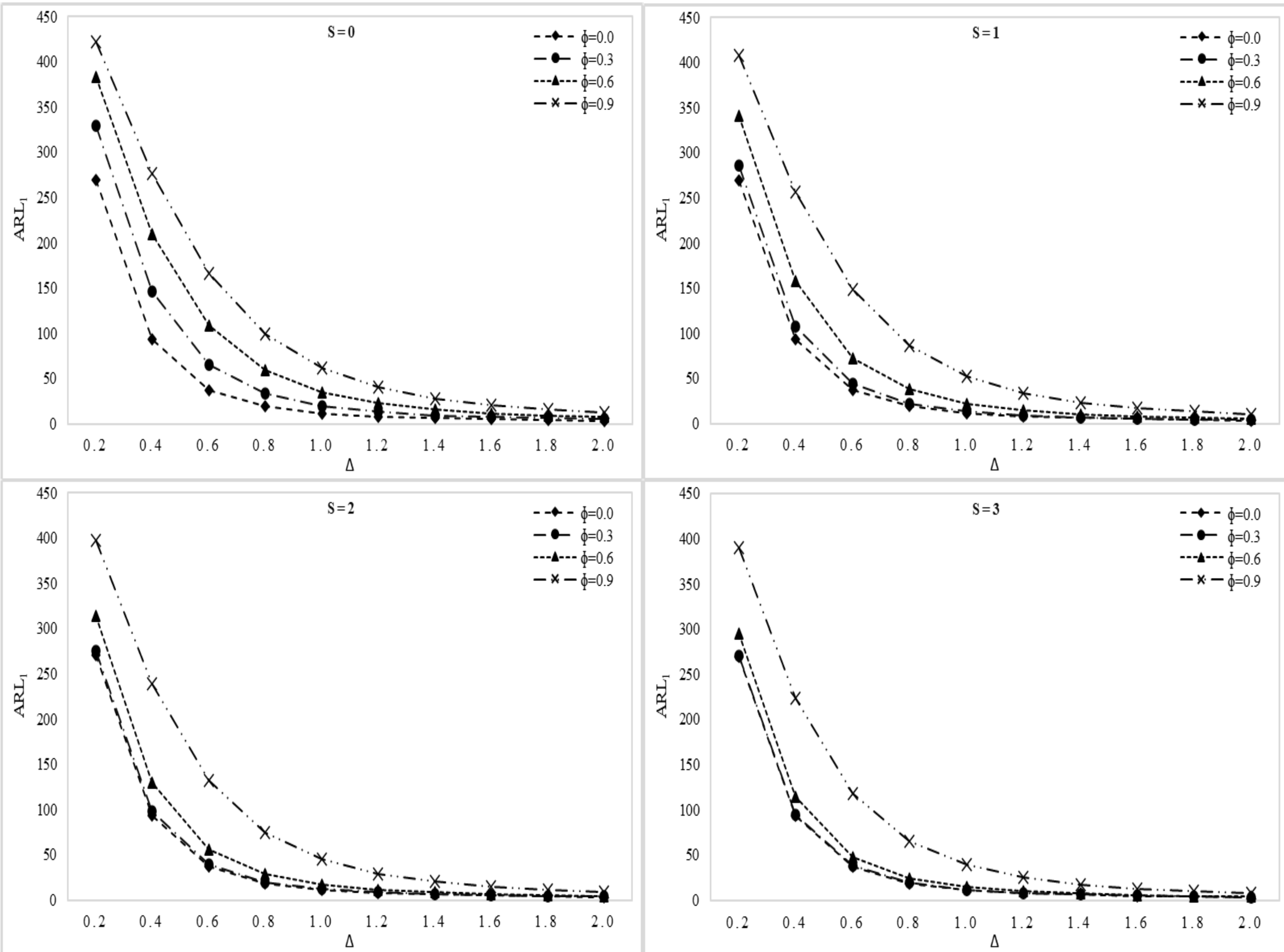


**FIGURE 4.** **Steady-state ARL Curves for DCCUSUM chart at s = 0, s = 1, s = 2 and s = 3.**

be sensitive enough to detect an unknown shift in a process parameter(s).

According to the argument, it would be more appropriate to assume that the shift occurs uniformly within a specified range, say, $\delta \in [a, b]$, Zhao et al. [10] proposed a DCUSUM chart to monitor a range of process mean shift where two different CUSUM charts work alongside. The DCUSUM chart performs better than the CUSUM and Shewhart-CUSUM charts at identifying mean shifts in ranges. A two-sided DCUSUM chart based on $\{\bar{X}_t\}$ includes two upper charts, $(A_{1,t}^+, A_{1,t}^-)$ and two lower $(A_{2,t}^+, A_{2,t}^-)$, at time $t$, that run concurrently:

$$\begin{Bmatrix} A_{r,t}^+ = max\left[0, +\left(\bar{X}_t - \mu_0\right) - K_r + A_{r,t-1}^+\right] \\ A_{r,t}^- = max\left[0, -\left(\bar{X}_t - \mu_0\right) - K_r + A_{r,t-1}^-\right] \end{Bmatrix} \quad (1)$$

where $A_{r,0}^+ = A_{r,0}^- = 0$ and $K_r (= k_r \frac{\sigma}{\sqrt{n}}, k_r > 0)$ is the reference parameters for $r = 1, 2$. The two-sided DCUSUM chart generates an OC signal whenever $A_{r,t}^+ > H_i$ or $A_{r,t}^- > H_r$, for $r = 1, 2$. The value of $H_r (= h_r \frac{\sigma}{\sqrt{n}}, h_r > 0)$ is chosen so that the in-control ARL of the DCUSUM chart reaches a specified level. The DCUSUM scheme requires the following assumptions to function effectively: (i) The shift magnitude $\delta$ occurs uniformly in $[a, b]$; (ii) $k_1 h_1 = k_2 h_2$ and $k_1 + h_1 > k_2 + h_2$; (iii) $k_1 = (3a + b)/8$ and $k_2 = (a + 3b)/8$. More details can refer to Zhao et al. [10].

### B. THE DCCUSUM CHART

To improve the sensitivity against the detection range and follow Zhao et al. [10]'s procedure, Haq and Bibi [11] proposed the DCCUSUM chart, which consists of two CCUSUM charts, one for detecting small-to-modest shifts and the other for modest-to-large shifts. It turns out that this chart is slightly more sensitive than the DCUSUM. The DCCUSUM chart starts by plotting the statistics of the two-sided CUSUM, say $(B_{1,t}, B_{2,t})$, based on $\bar{X}_t$, which is given by

$$\begin{Bmatrix} B_{r,t} = \left(\bar{X}_t - \mu_0 + B_{r,t-1}\right)\left(1 - \dfrac{K_r}{C_{r,t}}\right) & if\ C_{r,t} > K_r \\ B_{1,t} = 0 & if\ C_{r,t} \le K_r \end{Bmatrix} \quad (2)$$

**TABLE 5.** Zero- and Steady-state RARL, EQL, and PCI performance comparisons of the dual charts at s = 0, 1, 2, and 3.

| Chart → | | DCUSUM | | | | | | | | | |
|---|---|---|---|---|---|---|---|---|---|---|---|
| S↓ | ϕ→ | 0.0 | 0.1 | 0.2 | 0.3 | 0.4 | 0.5 | 0.6 | 0.7 | 0.8 | 0.9 |
| **Zero state** | | | | | | | | | | | |
| | RARL | 1.50 | 1.72 | 1.97 | 2.26 | 2.60 | 2.99 | 3.45 | 3.99 | 4.62 | 5.34 |
| 0 | EQL | 14.12 | 16.18 | 18.56 | 21.31 | 24.57 | 28.43 | 32.94 | 38.36 | 44.82 | 52.25 |
| | PCI | 1.34 | 1.54 | 1.76 | 2.02 | 2.33 | 2.70 | 3.13 | 3.64 | 4.25 | 4.96 |
| | RARL | 1.51 | 1.53 | 1.59 | 1.70 | 1.87 | 2.11 | 2.46 | 2.95 | 3.66 | 4.69 |
| 1 | EQL | 14.14 | 14.33 | 14.91 | 15.97 | 17.57 | 19.90 | 23.23 | 27.98 | 35.04 | 45.48 |
| | PCI | 1.34 | 1.36 | 1.41 | 1.52 | 1.67 | 1.89 | 2.20 | 2.65 | 3.32 | 4.31 |
| | RARL | 1.50 | 1.51 | 1.52 | 1.56 | 1.64 | 1.78 | 2.02 | 2.40 | 3.04 | 4.16 |
| 2 | EQL | 14.12 | 14.14 | 14.27 | 14.67 | 15.42 | 16.74 | 18.98 | 22.65 | 28.92 | 40.12 |
| | PCI | 1.34 | 1.34 | 1.35 | 1.39 | 1.46 | 1.59 | 1.80 | 2.15 | 2.74 | 3.81 |
| | RARL | 1.51 | 1.50 | 1.51 | 1.52 | 1.56 | 1.64 | 1.79 | 2.08 | 2.63 | 3.74 |
| 3 | EQL | 14.14 | 14.14 | 14.17 | 14.28 | 14.64 | 15.37 | 16.86 | 19.62 | 24.93 | 35.90 |
| | PCI | 1.34 | 1.34 | 1.34 | 1.35 | 1.39 | 1.46 | 1.60 | 1.86 | 2.37 | 3.41 |
| **Steady state** | | | | | | | | | | | |
| | RARL | 1.46 | 1.67 | 1.92 | 2.20 | 2.52 | 2.91 | 3.36 | 3.89 | 4.51 | 5.23 |
| 0 | EQL | 13.63 | 15.63 | 17.90 | 20.58 | 23.72 | 27.50 | 31.95 | 37.21 | 43.50 | 50.95 |
| | PCI | 1.29 | 1.48 | 1.70 | 1.95 | 2.25 | 2.61 | 3.03 | 3.53 | 4.13 | 4.83 |
| | RARL | 1.46 | 1.48 | 1.54 | 1.65 | 1.82 | 2.05 | 2.39 | 2.87 | 3.57 | 4.58 |
| 1 | EQL | 13.64 | 13.82 | 14.39 | 15.40 | 16.95 | 19.21 | 22.42 | 27.10 | 33.98 | 44.20 |
| | PCI | 1.29 | 1.31 | 1.37 | 1.46 | 1.61 | 1.82 | 2.13 | 2.57 | 3.22 | 4.19 |
| | RARL | 1.46 | 1.46 | 1.48 | 1.51 | 1.59 | 1.73 | 1.96 | 2.33 | 2.96 | 4.06 |
| 2 | EQL | 13.67 | 13.66 | 13.78 | 14.14 | 14.88 | 16.17 | 18.30 | 21.89 | 27.99 | 38.94 |
| | PCI | 1.30 | 1.30 | 1.31 | 1.34 | 1.41 | 1.53 | 1.74 | 2.08 | 2.66 | 3.69 |
| | RARL | 1.46 | 1.46 | 1.46 | 1.48 | 1.51 | 1.59 | 1.74 | 2.02 | 2.56 | 3.65 |
| 3 | EQL | 13.65 | 13.64 | 13.67 | 13.79 | 14.11 | 14.85 | 16.26 | 18.93 | 24.09 | 34.79 |
| | PCI | 1.30 | 1.29 | 1.30 | 1.31 | 1.34 | 1.41 | 1.54 | 1.80 | 2.29 | 3.30 |
| **Chart →** | | **DCCUSUM** | | | | | | | | | |
| **Zero state** | | | | | | | | | | | |
| | RARL | 1.48 | 1.69 | 1.93 | 2.22 | 2.54 | 2.93 | 3.37 | 3.91 | 4.52 | 5.23 |
| 0 | EQL | 13.88 | 15.87 | 18.17 | 20.89 | 24.06 | 27.81 | 32.22 | 37.56 | 43.78 | 51.15 |
| | PCI | 1.32 | 1.51 | 1.72 | 1.98 | 2.28 | 2.64 | 3.06 | 3.56 | 4.15 | 4.85 |
| | RARL | 1.47 | 1.50 | 1.56 | 1.66 | 1.83 | 2.07 | 2.41 | 2.89 | 3.58 | 4.58 |
| 1 | EQL | 13.86 | 14.06 | 14.64 | 15.65 | 17.22 | 19.49 | 22.72 | 27.44 | 34.30 | 44.45 |
| | PCI | 1.31 | 1.33 | 1.39 | 1.48 | 1.63 | 1.85 | 2.16 | 2.60 | 3.25 | 4.22 |
| | RARL | 1.47 | 1.48 | 1.49 | 1.53 | 1.61 | 1.75 | 1.97 | 2.35 | 2.98 | 4.07 |
| 2 | EQL | 13.86 | 13.90 | 14.01 | 14.37 | 15.11 | 16.43 | 18.59 | 22.19 | 28.31 | 39.24 |
| | PCI | 1.31 | 1.32 | 1.33 | 1.36 | 1.43 | 1.56 | 1.76 | 2.11 | 2.69 | 3.72 |
| | RARL | 1.47 | 1.47 | 1.48 | 1.49 | 1.53 | 1.60 | 1.76 | 2.04 | 2.58 | 3.66 |
| 3 | EQL | 13.87 | 13.85 | 13.89 | 14.02 | 14.35 | 15.07 | 16.51 | 19.22 | 24.39 | 35.10 |
| | PCI | 1.32 | 1.31 | 1.32 | 1.33 | 1.36 | 1.43 | 1.57 | 1.82 | 2.31 | 3.33 |
| **Steady state** | | | | | | | | | | | |
| | RARL | 1.46 | 1.67 | 1.91 | 2.19 | 2.52 | 2.90 | 3.34 | 3.86 | 4.47 | 5.19 |
| 0 | EQL | 13.66 | 15.65 | 15.65 | 20.58 | 23.74 | 27.46 | 31.87 | 37.06 | 43.21 | 50.59 |
| | PCI | 1.30 | 1.48 | 1.48 | 1.95 | 2.25 | 2.61 | 3.02 | 3.52 | 4.10 | 4.80 |
| | RARL | 1.46 | 1.48 | 1.54 | 1.64 | 1.81 | 2.04 | 2.38 | 2.86 | 3.54 | 4.54 |
| 1 | EQL | 13.65 | 13.85 | 14.40 | 15.42 | 16.98 | 19.19 | 22.41 | 27.06 | 33.83 | 43.93 |
| | PCI | 1.30 | 1.31 | 1.37 | 1.46 | 1.61 | 1.82 | 2.13 | 2.57 | 3.21 | 4.17 |
| | RARL | 1.46 | 1.46 | 1.47 | 1.51 | 1.59 | 1.73 | 1.95 | 2.32 | 2.95 | 4.03 |
| 2 | EQL | 13.66 | 13.67 | 13.81 | 14.17 | 14.89 | 16.18 | 18.32 | 21.87 | 27.97 | 38.79 |
| | PCI | 1.30 | 1.30 | 1.31 | 1.34 | 1.41 | 1.54 | 1.74 | 2.07 | 2.65 | 3.68 |
| | RARL | 1.46 | 1.46 | 1.46 | 1.47 | 1.51 | 1.58 | 1.74 | 2.02 | 2.55 | 3.63 |
| 3 | EQL | 13.65 | 13.67 | 13.70 | 13.81 | 14.51 | 14.87 | 16.28 | 18.95 | 24.07 | 34.68 |
| | PCI | 1.30 | 1.30 | 1.30 | 1.31 | 1.38 | 1.41 | 1.54 | 1.80 | 2.28 | 3.29 |

where $C_{r,t} = |\bar{X}_t - \mu_0 + B_{r,t-1}|$ with $B_{r,0} = 0$ for $r = 1, 2$. Here $K_r = k_r \frac{\sigma}{\sqrt{n}}$ and $H_r = h_r \frac{\sigma}{\sqrt{n}}$, for $r = 1, 2$, are the slack/sensitive parameters and decisions intervals of the DCCUSUM chart, respectively. As it can be seen that $B_{1,t}$ and $B_{2,t}$ are the two different plotting-statistics which are used to operate the DCCUSUM charts more effectively. Whenever either $B_{r,t} > H_r$ and/or $B_{r,t} < -H_r$, the DCCUSUM generates an OC signal. This chart works with the same assumptions as discussed for the DCUSUM chart, see for further details in Haq and Bibi [11].

## III. DUAL CHARTS FOR THE AR (1) PROCESS WITH S-SKIPPING SAMPLING SCHEME

Let $\{Y_{t,i}\}$, $i = 1, 2, \ldots, n$ be a sequence of samples from the stationary AR(1) model that fits the autocorrelated normal distribution $N(\mu_0, \sigma_0)$ at $t \geq 1$, given by

$$Y_{t,i} - \mu_0 = \phi \left(Y_{t,i-1} - \mu_0\right) + \varepsilon_i, \tag{3}$$

where $Y_{t,i}$ is the current measurement of the quality characteristic of the time series, which depends on the previous measurement, $Y_{t,i-1}$. $\phi$ ($|\phi| < 1$) is a specified parame-

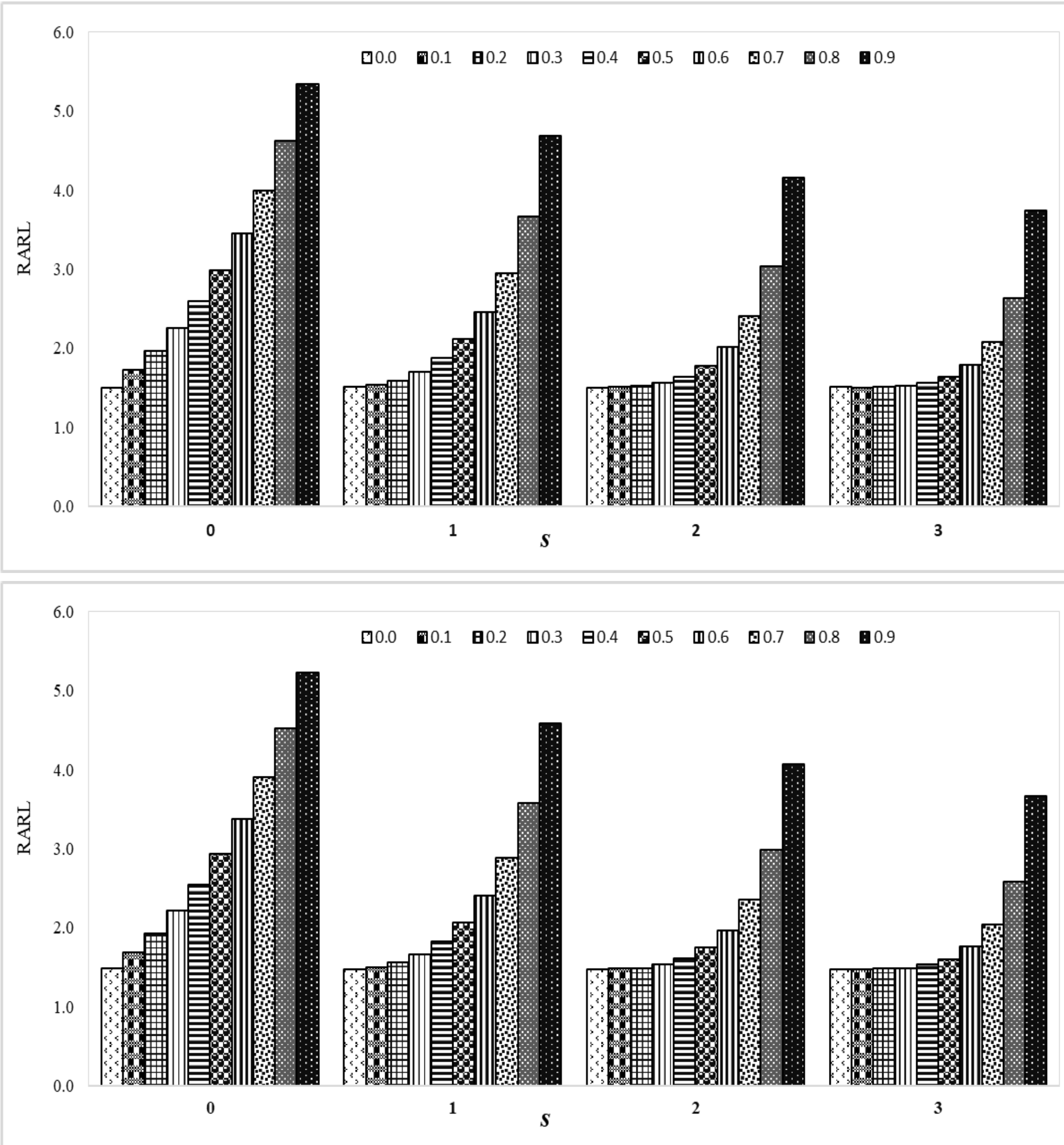


**FIGURE 5.** Zero-state RARL comparison for DCUSUM and DCCUSUM Charts at s = 0, 1, 2 and 3.

ter which is also called as a level of autocorrelation. Mean $\mu_0$ and the standard deviation $\sigma_0$, are the IC process parameter and $\varepsilon_t$ is iid $(0, \sigma_\varepsilon)$ normal random variable – see Alwan and Radson [33]. When assignable causes are present, the process mean changes from $\mu_0$ to $\mu_1 = \mu_0 + \delta\sigma_0$, resulting in $\delta = \mu_1 - \mu_0/\sigma_0$.

Let $\bar{Y}_t = \sum_{i=1}^{n} Y_{t,i}/n$ indicate the charting-statistic at $t$ sampling point. The sampled observations are autocorrelated, which means that there is dependence within the computation of $\bar{Y}_t$ and at the same time, $\bar{Y}_i$ and $\bar{Y}_j (i \neq j)$ are independent, indicating no cross-correlation.

It has been established that sampling methods of skipping some of the succeeding observations can reduce serial dependence in time series data. Considering Gilbert et al. [34]'s advice in contradiction of using high skipping values, the use of skipping $s(= 1, 2, 3)$ consecutive sample(s) was suggested by Costa and Castagliola [17] as a strategy to lessen serial dependence on the Shewhart $\bar{X}$ monitoring schemes. The corresponding $s$-skipping sampling strategy process is therefore remains an AR(1) process, however is defined as $\{Y_{t,i} : t \geq 1; i = 1, s+2, 2s+3, 3s+4, \ldots\}$ with parameter $\phi^{s+1}$:

$$Y_{t,i} - \mu_0 = \phi^{s+1}\left(Y_{t,i-s-1} - \mu_0\right) + \varepsilon'_i \tag{4}$$

with $\varepsilon'_i = \varepsilon_i + \phi\varepsilon_{i-1} + \phi^2\varepsilon_{i-2} + \ldots + \phi^s\varepsilon_{i-s}$. The plotting-statistic (mean) is $\bar{Y}_t = \frac{1}{n}\sum_{i=1}^{n} Y_{t,(s+1)i-s}$, at $t$ sampling point and the standard deviation in Eq. (4) is given by

$$\sigma\left(\bar{Y}_t\right) = \frac{\sigma_0}{\sqrt{n}C_2(n, s, \phi)}, \tag{5}$$

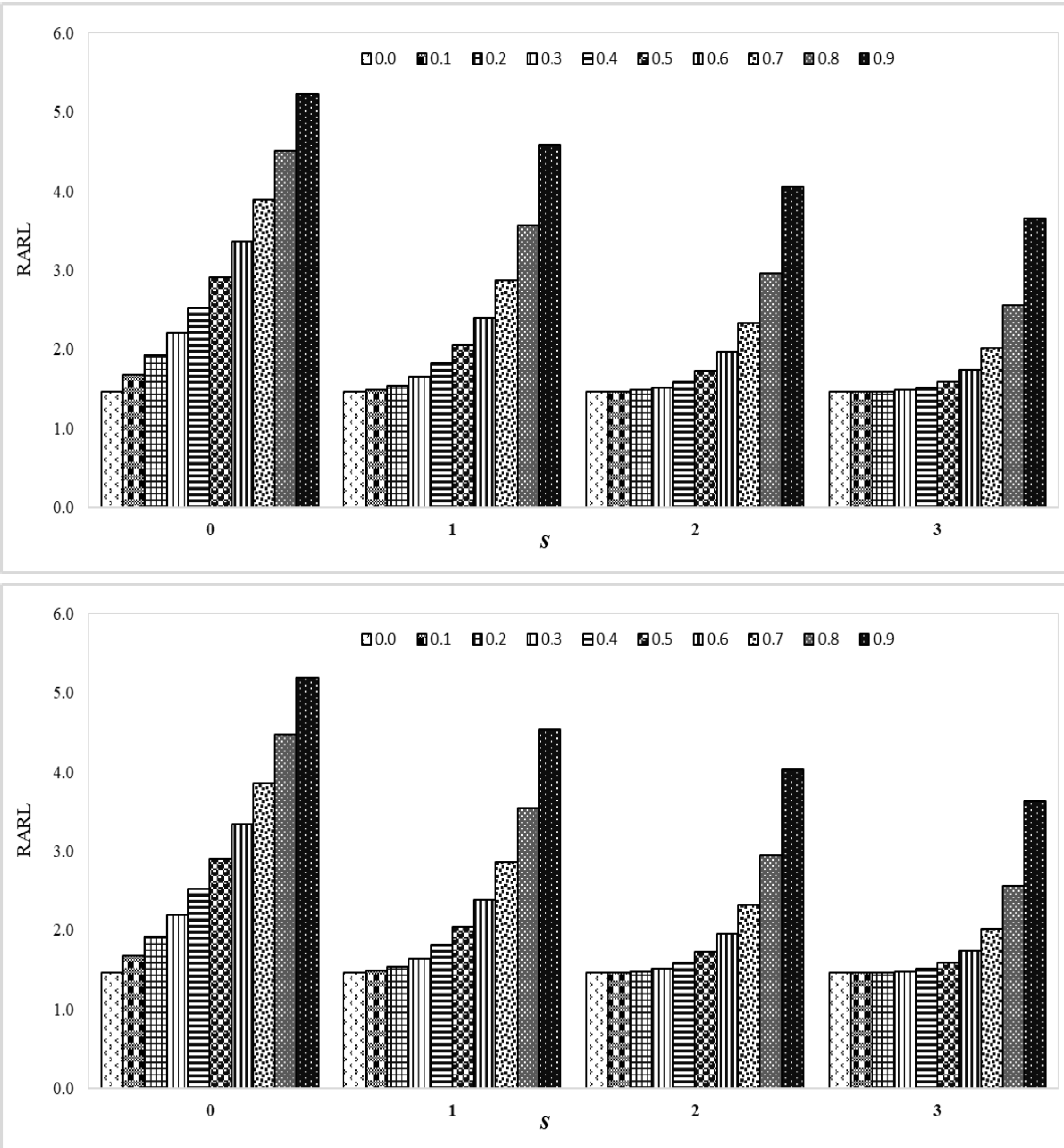


**FIGURE 6.** Steady-state RARL comparison for DCUSUM and DCCUSUM Charts at s = 0, 1, 2 and 3.

where

$$\sqrt{n}C_2\left(n,s,\phi\right)=\sqrt{\frac{n}{n+2\left[\frac{\phi^{(s+1)(n+1)}-n\phi^{2s+2}+(n-1)\phi^{s+1}}{\left(\phi^{s+1}-1\right)^2}\right]}}. \quad (6)$$

We investigate how the dual CCs perform when autocorrelation is present in the following sections.

### A. THE DCUSUM CHARTS FOR AUTOCORRELATED PROCESS

To deal with autocorrelated processes, a DCUSUM CC is presented. Two upper and two lower statistics are respectively given as $(D_{r,t}^{+}, D_{r,t}^{-})$ by using the order of $\bar{Y}_t$ in Eq. (1). The DCUSUM mean chart is given bellow.

$$\left\{\begin{matrix} \boldsymbol{D_{r,t}^{+}} = \boldsymbol{max}\left[0, +\left(\bar{X}_t-\boldsymbol{\mu_0}\right)-\boldsymbol{K_r}+\boldsymbol{D_{r,t-1}^{+}}\right] \\ \boldsymbol{D_{r,t}^{-}} = \boldsymbol{max}\left[0, -\left(\bar{X}_t-\boldsymbol{\mu_0}\right)-\boldsymbol{K_r}+\boldsymbol{D_{r,t-1}^{-}}\right] \end{matrix}\right\} \quad (7)$$

where $D_{r,0}^{+} = D_{r,0}^{-} = 0$ and $K_r(= k_r\frac{\sigma}{\sqrt{n}}; k_r > 0)$ is the sensitive parameter of the DCUSUM chart for $r = 1, 2$. An OC signal is produced by a two-sided DCUSUM chart for the detection of an increase or decrease in the process mean when $D_{r,t}^{+} > H_r$ or $D_{r,t}^{-} > H_r$, for $r = 1, 2$, where $H_r$ $(= h_r\frac{\sigma}{\sqrt{n}}; h_r > 0)$, is the control limit, respectively. This CC also works with the same constraints as discussed in Subsection (2.1).

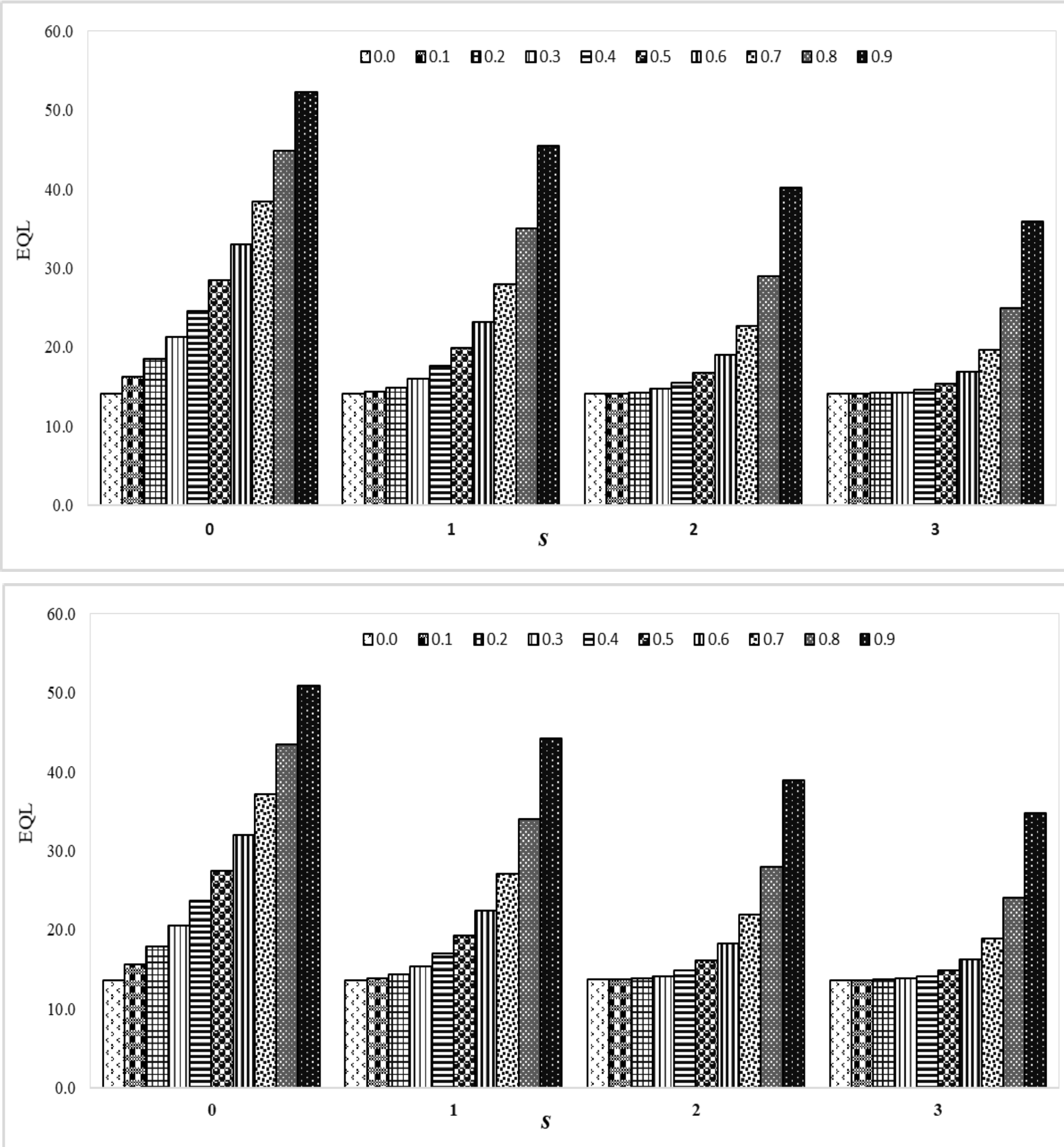


**FIGURE 7.** Zero-state EQL comparison for DCUSUM and DCCUSUM Charts at s = 0, 1, 2 and 3.

### B. THE DCCUSUM CHARTS FOR AUTOCORRELATED PROCESS

The DCCUSUM control chart for monitoring the mean in the presence of autocorrelation, has been studied in this subsection.

Using the sequence $\{\bar{Y}_t\}$ based on the model in Eq. (4), the plotting two upper statistics $(E_{1,t}^{+}, E_{2,t}^{+})$ and two lower statistics $(E_{1,t}^{-}, E_{2,t}^{-})$ of the DCCUSUM mean chart are given by:

$$\begin{Bmatrix} E_{r,t} = \left(\bar{X}_t - \mu_0 + E_{r,t-1}\right)\left(1 - \frac{K_r}{C_{r,t}}\right) & if\ F_{r,t} > K_r \\ E_{1,t} = 0 & if\ F_{r,t} \leq K_r \end{Bmatrix} \quad (8)$$

where the starting values for the statistics are $E_{r,0} = 0$, $r = 1, 2$ with $F_{r,t} = |\bar{Y}_t - \mu_0 + E_{r,t-1}|$. $K_1$ and $K_2$ are the sensitive parameters of the DCCUSUM chart and if the plotting-statistics go over the threshold limits $H_1$ and $H_2$, $E_{r,t} > H_r$ and/or $E_{r,t} < -H_r$, where $r = 1, 2$, then the process is considered to be OC, and the rest of the DCCUSUM chart's description is the same as presented in the Subsection (2.2).

## IV. SENSITIVE MEASURES AND COMPARATIVE ANALYSES

This section conducts detailed investigations for both the DCUSUM and DCCUSUM charts in the presence of

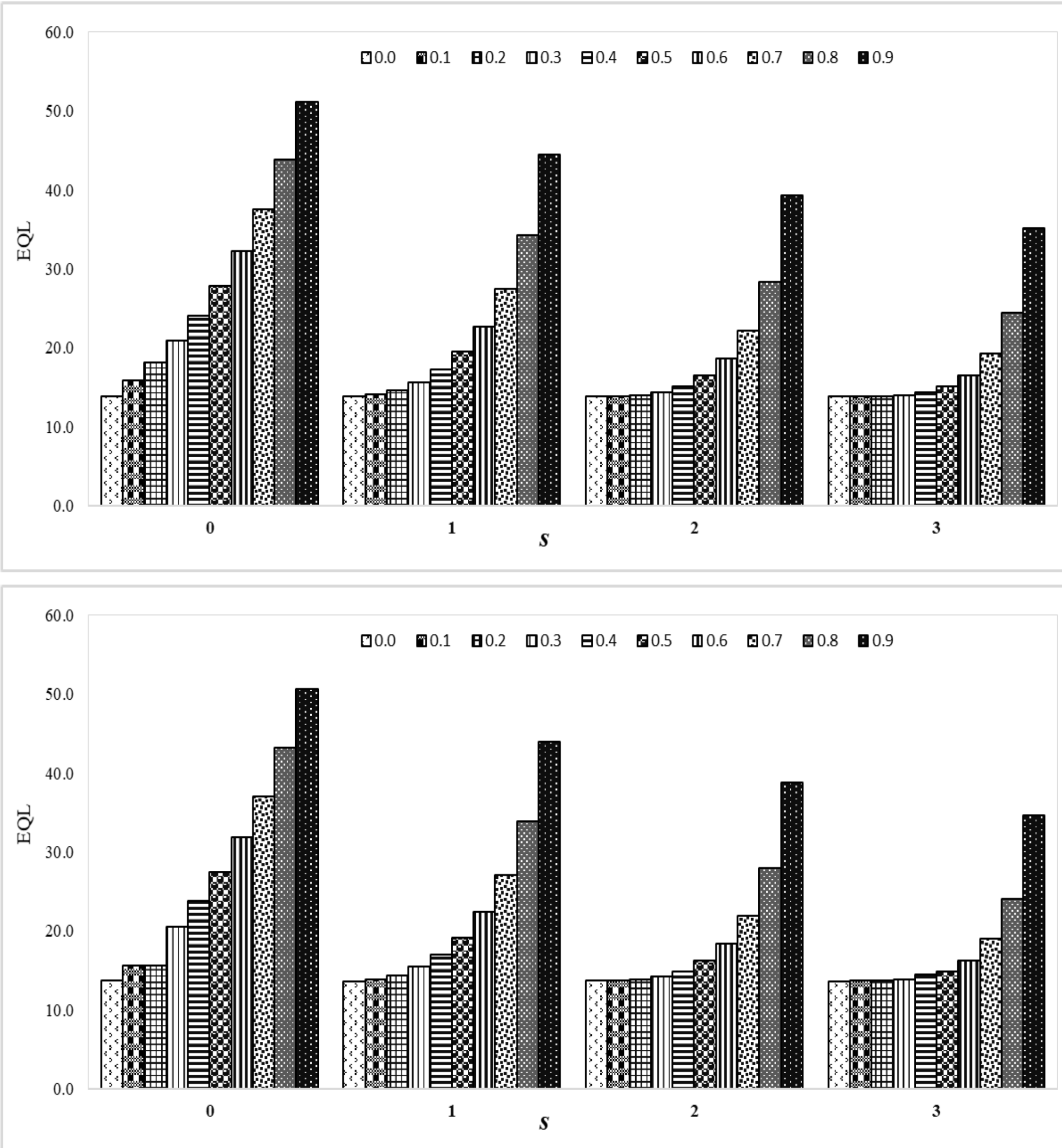


**FIGURE 8.** Steady-state EQL comparison for DCUSUM and DCCUSUM Charts at s = 0, 1, 2 and 3.

autocorrelated observations. This comparative analysis aims to demonstrate how autocorrelated observations have a significant impact on the performance of the aforementioned charts when monitoring a variety of process mean shifts. Measures commonly used in SPC to evaluate the performance profiles of control charts, such as the ARL and SDRL, are used to evaluate the performance sensitivity of a CC for a given specific size of shift. When the shift is unknown and can be reasonably assumed to be within a certain range. In this case, it is appropriate to consider the measures capable of providing the overall range of performance. These are the well-established performance measures in the SPC literature, namely the EQL, RARL, and PCI. The measures are computed using Monte Carlo simulations with the developed algorithms in RStudio 4.1.2 (R Foundation for Statistical Computing). Interpretations of these measures are given as follows:

1) **ARL and SDRL:** The average of the run length distribution is usually used to analyses a chart. A run is a collection of samples that the process remains IC. The ARL is typically defined as the reciprocal of the probability that a statistic used for process monitoring would fall outside the control limits. When a process is either IC or OC, it refers to the number of samples taken before a shift is noticed. For the purposes of

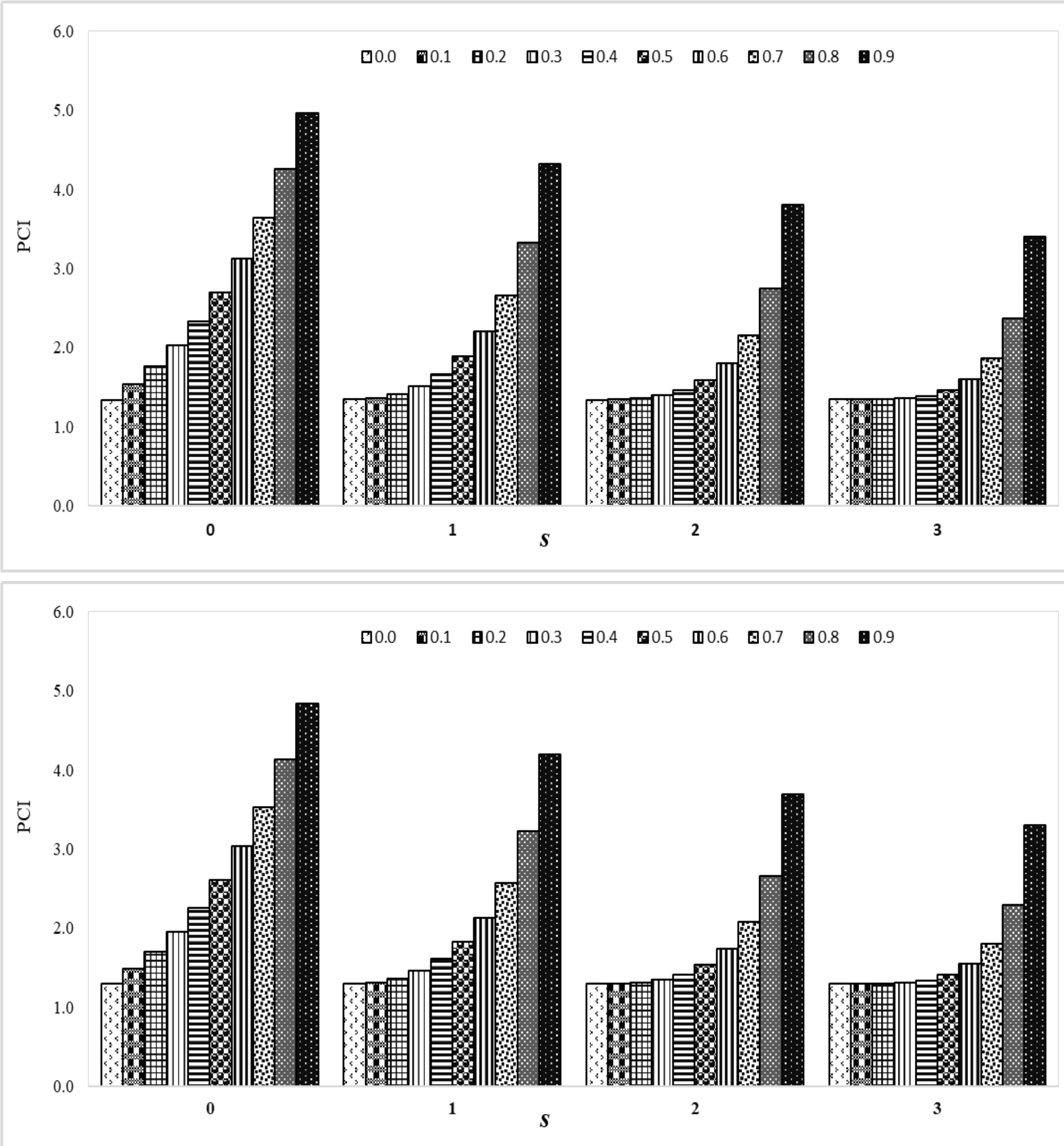


**FIGURE 9.** Zero-state PCI comparison for DCUSUM and DCCUSUM Charts at s = 0, 1, 2 and 3.

computing ARL, it is assumed that the process has been in IC from its starting value, which is referred to as the zero-state ARL (ZSARL). Another type of the ARL is calculated by supposing that the process has been running for a long time when the monitoring scheme is applied, implying that the scheme's starting value may not be zero, resulting in the steady-state ARL (SSARL). The SDRL measures the spread in the run length distribution. When the process is IC or OC, it is preferable to have low SDRL values.

2) **EQL:** The EQL measures a CC's overall effectiveness against a range of shifts. It is a weighted average of the ARLs over the entire mean shift domain, for example $[a, b]$, using $\delta_j^2$ as a weight function. The following formula is used to calculate the EQL:

$$EQL \approx \frac{1}{m+1} \sum\nolimits_{j=0}^{m} \delta_j^2 ARL\left(\delta_j\right), \tag{9}$$

where $a$ is the minimum and $b$ is the maximum bound of the mean shift $\delta$. The lower the EQL value, the greater the control chart's detection capabilities when $(a \leq \delta \leq b]$. The EQL values are calculated by integrating across the entire shift domain, and the integration can be assessed numerically.

3) **RARL:** To evaluate the run length performance of CCs, it can also be used an alternative performance metric RARL, which describes the effectiveness of a CC over the entire process shift domain $(a \leq \delta \leq b]$, see for

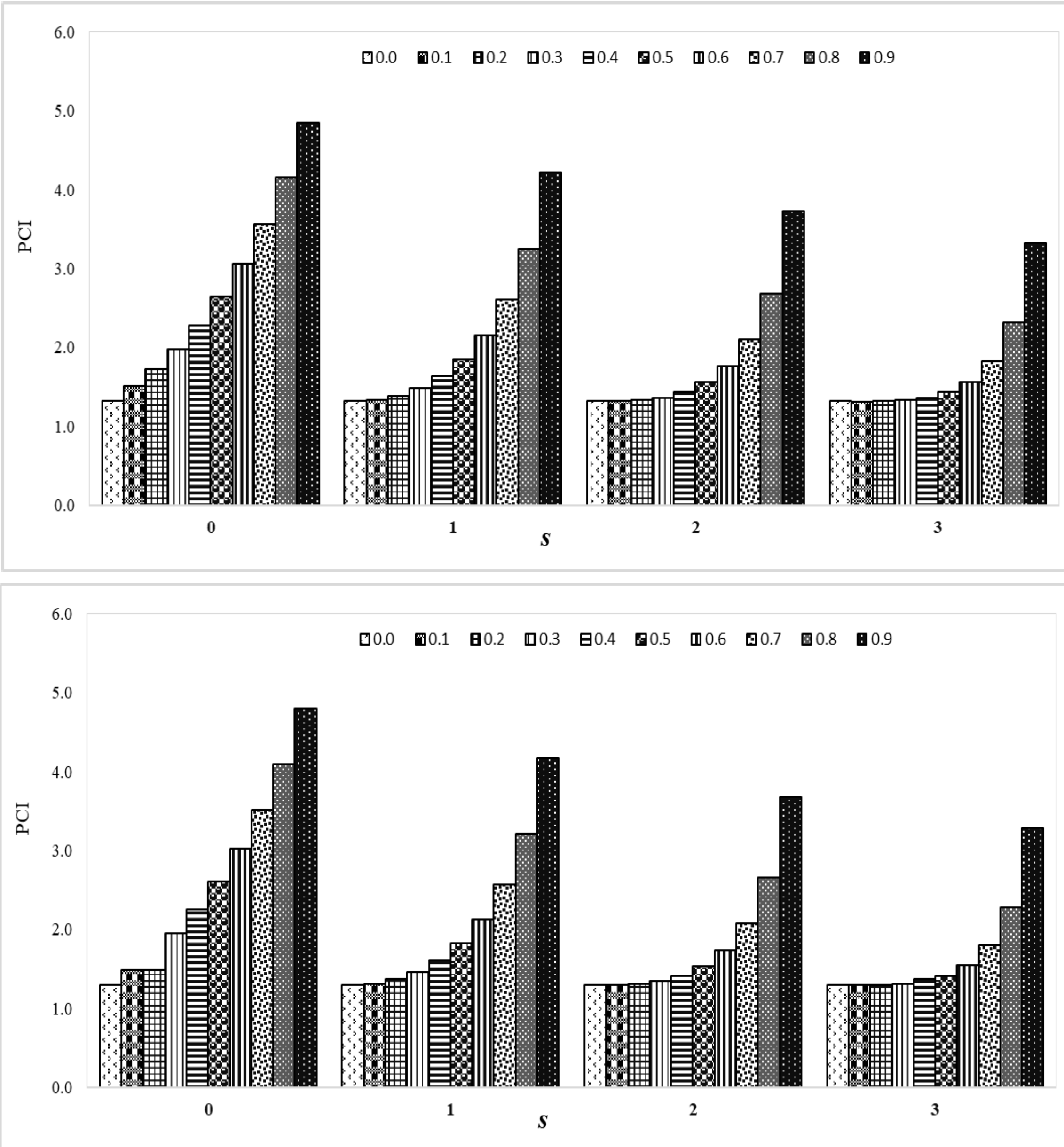


**FIGURE 10.** Steady-state PCI comparison for DCUSUM and DCCUSUM Charts at s = 0, 1, 2 and 3.

example, Zhao et al. [10] and Wu et al. [35]. The RARL can be expressed in a discrete form as follows:

$$RARL \approx \frac{1}{m+1}\sum\nolimits_{j=0}^{m}\frac{ARL_c\left(\delta_j\right)}{ARL_{opt}\left(\delta_j\right)}, \qquad (10)$$

and $\delta_j = a+j(b-a)/m$, where $m$ is a specified number. The RARL value for the underlying optimal CUSUM chart (OCC) is 1, as expected, and all the charts are compared to the OCC. In comparison to the OCC, the smaller the RARL value for a given range of the mean shift, the more powerful the control chart (compared chart) is in detecting the process shifts over the range.

4) **PCI:** PCI is the ratio of competing and optimum charts' EQL values under the same conditions. It assists in the evaluation of performance by completing an EQL ranking. The PCI value for the chart with the lowest EQL is one, while the PCI value for other charts is more than one. This could be mathematically formulated as:

$$PCI \approx \frac{EQL}{EQL_{OCC}}. \qquad (11)$$

Many authors, including, (Zhao et al. [10]; Ahmad et al. [35]), employ the above performance indicators in their research works.

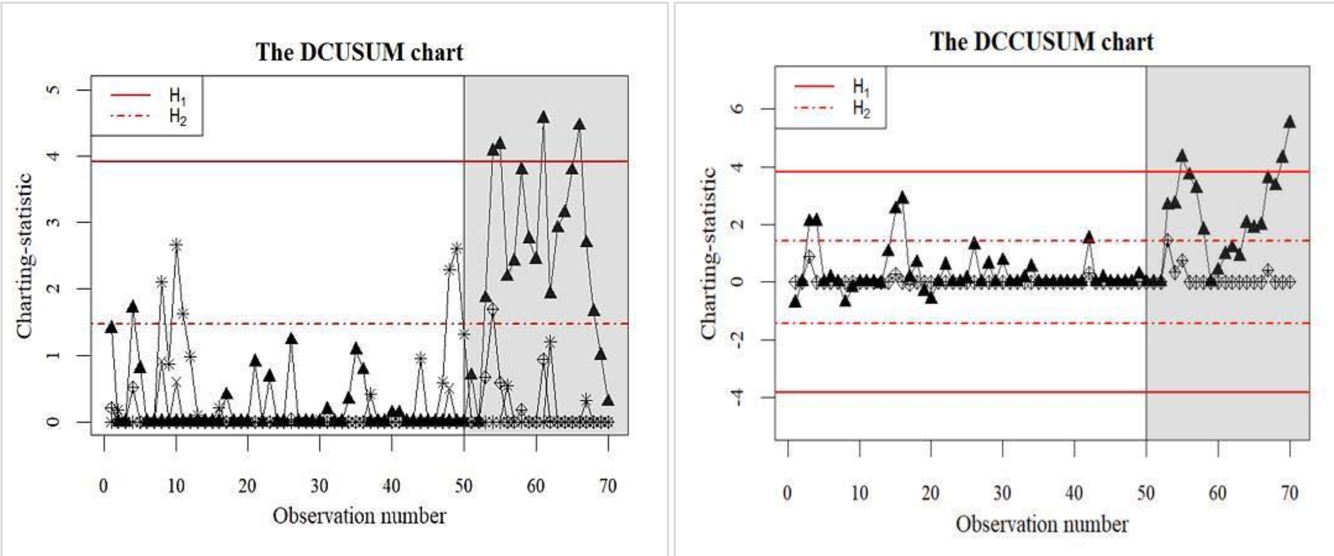


FIGURE 11. Control charts for DCUSUM and DCCUSUM charts at $\phi = 0.0$.

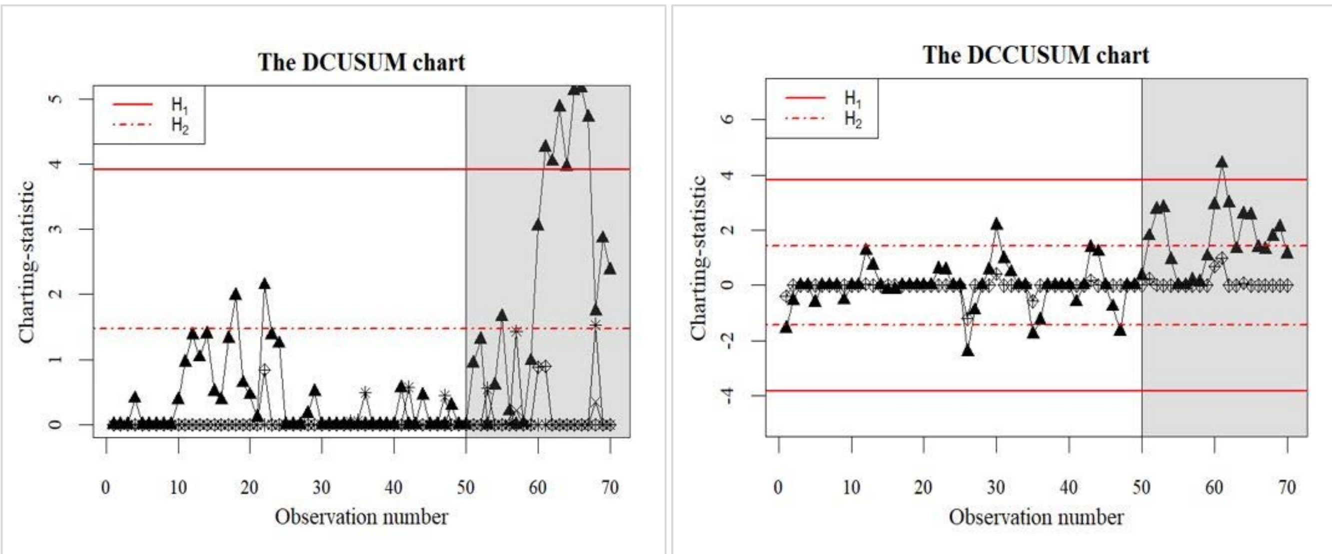


FIGURE 12. Control charts for DCUSUM and DCCUSUM charts at $\phi = 0.5$.

## A. EVALUATION

The performance of the two-sided dual CUSUM charts for a specific shift size is evaluated in terms of the ARL and SDRL in the presence and absence of autocorrelation. For the sake of brevity, on the lines of Zhao et al. [10], the range [0.25, 5.0] is considered for different sizes of shifts in a range in the process's mean parameter and the $ARL_0$ of different charts are matched at 500 for both the ZSARL and SSARL profiles, respectively. Other measures, EQL, RARL and PCI, are calculated to observe the overall performance of the CCs with the help of the ARL values.

The level of autocorrelation, notation $\phi$, are set between 0 and 1 with an increment of 0.1, the $ARL_1$ performance of the corresponding charts are estimated. Here, $\phi = 0$ denotes an ongoing process with no autocorrelation, while $\phi = 1$ denotes the worst-case scenario. The $s$-skipping sampling strategy is used as a remedial measure to compensate for the negative effect of autocorrelation by incorporating different non-neighbouring item settings, such as $s = 0, 1, 2, 3$. Before the mean shifts happen in a process, the SSARL is based on 32 samples, see Lucas and Crosier [8]. The values of $k_1$ and $k_2$ in the DCUSUM and DCCUSUM charts are the lower and upper quartiles of the range $[a/2, b/2]$, $k_1 = (3a + b)/8$ and $k_2 = (a + 3b)/8$, respectively.

The simulation results are computed using the Monte Carlo approach with 100,000 replications from a standard normal distribution of a particular size for each random sample. The generated replications are used to calculate the run length profiles.

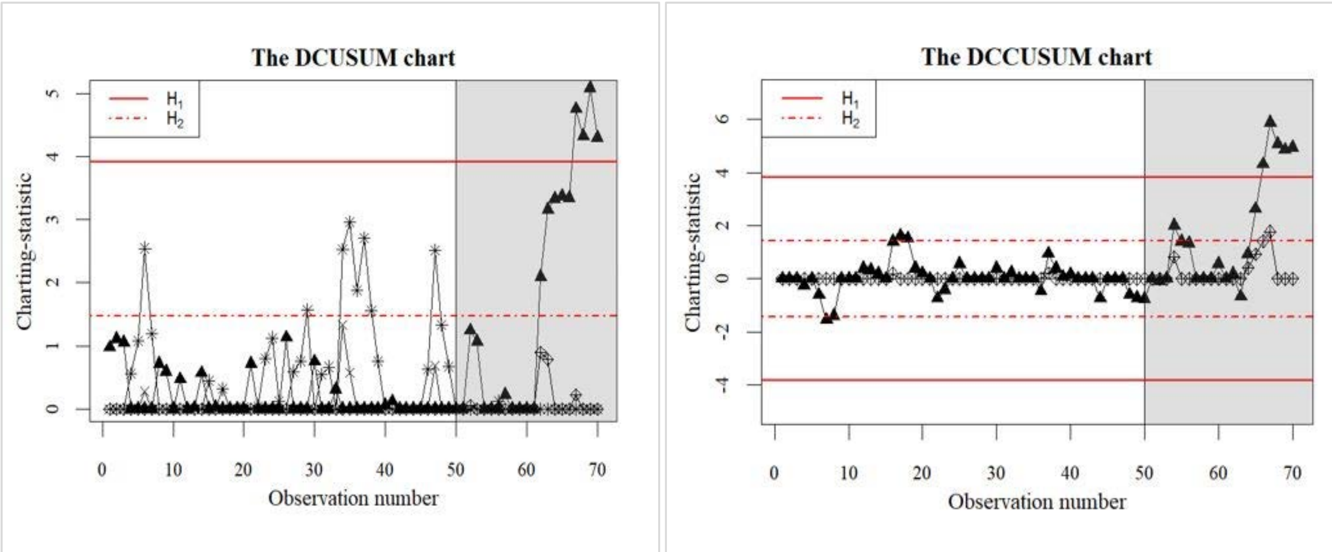


**FIGURE 13. Control charts for DCUSUM and DCCUSUM charts at $\phi = 0.9$.**

At various values of $s$ and $\phi$, the run length profiles ($ARL_1$ & SDRL) for the ZSARL and SSARL for a certain shift size are reported in Tables 1-4. The ARL curves (Figs. 1-4) are employed to show how well charts perform when autocorrelation is present. Figs. 5-10 show the EQL, RARL, and PCI values, which can be used to assess the charts' overall performance.

These figures show how autocorrelation affects the performance of the dual charts and how the $s$-skipping strategy remedy reduce this negative effect. The following are the main findings:

1) **Shift $\delta$ ↑ then ARL/SDRL ↓**: From Tables 1-4, it can be shown that as shift increases from 0.2 to 2.0, the $ZSARL_1$ and $SSARL_1$ values of the DCUSUM and DCCUSUM charts drop at any value of $s$ (0 to 3) and $\phi$ (0.0 to 0.9), respectively. The ARL/SDRL is inversely proportional to the shift size when the $ARL_0$ is fixed. For example, Table 1 shows ($\delta$, $ARL_1$) as (0.20, 271.37), (1.00, 11.92), and so on (2.00, 3.59). The results show a similar declining behavior of SDRL values. For example, Table 1 shows ($\delta$, SDRL) as (0.20, 267.01), (1.00, 8.03), and so on (2.00, 1.58). For $s = 0, 1, 2, 3$ and $\phi$ (0.0 to 0.9), the same falling trend of $ARL_1$ curves can be seen in Figs. 1-4 with the increase of $\delta$.
2) **Level $\phi$ ↑ then ARL/SDRL ↑**: Tables 1-4 show that as the amount of $\phi$ increases from 0 (no autocorrelation scenario, say iid) up 0.9, the $ZSARL_1$ and $SSARL_1$ values of DCUSUM and DCCUSUM charts (at $s = 0, 1, 2,$ and 3) have an increasing trend. The OC ARL ($ARL_1$) is proportional to the level $\phi$, meaning that the higher the autocorrelation, the higher the $ARL_1$. For example, we can see ($\phi$, $ARL_1$) from Table 2 as (0.00, 93.18), (0.30, 146.46), (0.60, 211.32), and so on(0.9, 279.98) at $\delta = 0.4$ with $s = 0$. The left bottom curve in Figs. 1-4 is for $\phi = 0.0$ while the right uppermost curve is for $\phi = 0.9$. The $ARL_1$ curves, in general, tilt upwards to the right as the $\phi$ value increases and decreases as the value of $s$ increases. As the level of $\phi$ rises, the SDRL values rise as well. For example, Table 3 shows ($\phi$, SDRL) as (0.0, 271.12), (0.3, 332.17), (0.6, 383.85), and so on (0.9, 424.32) at $\delta = 0.4$ with $s = 0$. Table 1, Table 2, and Table 4 and show that ARL and SDRL values (with respect to $\phi$) have similar behaviour.
3) **Level $s$ ↑ then ARL/SDRL ↓**: The $s$-skipping sampling was used to reduce autocorrelation and hence lower the $ZSARL_1$ and $SSARL_1$ of both the DCUSUM and DCCUSUM charts. This can be seen in Tables 1-4. That is, for instance, values from Table 2 in pair form are reported here, ($s$, [$ARL_1$(SDRL)])∈ {(0, [366.77(365.48)]), (1, [323.81(321.92)]), (2, [300.94 (299.98)]), (3, [286.55(284.91)])} and Table, for $\phi = 0.5$ at $\delta = 0.2$, (0, [366.48 (364.64)]), (1, [317.80 (314.77)]), (2, [296.12 (293.48)]), (3, [283.03 (279.81)]). The phenomena is also supported by the results in Figs. 5-10.
4) **Level $\phi$ ↑ then EQL/RARL/PCI ↑**: In Table 5, the overall zero-state and steady-state performance of the DCUSUM and DCCUSUM charts are presented and can also be observed from Figs. 5-10. For example, one may observe ($\phi$, EQL) at $s = 0$ for the DCUSUM chart as (0.0, 14.12), (0.30, 21.31), (0.60, 32.94) and (0.9, 52.25) while for the DCCUSUM chart, they are (0.0, 13.88), (0.30, 20.89), (0.60, 32.22) and (0.9, 51.15), respectively.
5) **Level $s$ ↑ then EQL/RARL/PCI ↓**: It can be observed from the Table 5 and Figs. 5-10 that the EQL, RARL and PCI values of each chart decrease as the value of $s$ increases, which shows that the overall effectiveness of a chart is directly proportional to the number of $s$.

For instance, it may be observed that (at $\phi = 0.9$, $s = 0, 1, 2, 3$), the respective EQL values for the DCUSUM chart are 52.25, 45.48, 40.12, and 35.9, and for the DCCUSUM chart, are 51.15, 44.45, 39.24, and 35.1. On the similar lines for other overall measures, (RARL, PCI) are (5.34, 4.96), (4.69, 4.31), (4.16, 3.81), and (3.74, 3.41) for the DCUSUM chart, as well as they are (5.23, 4.85), (4.58, 4.22), (4.07, 3.72), and (3.66, 3.33) for the DCCUSUM chart, respectively.

6) **Sensitivity based preference**: In the presence of autocorrelation, all the results reported in tables or shown in the figures demonstrate that the DCCUSUM chart is slightly more sensitive than the DCUSUM charts in the zero-state and steady-state, with or without applying the skipping strategy to both charts.

## V. AN ILLUSTRATIVE EXAMPLE (APPLICATION OF STUDY)

In this example, a simulated dataset with different levels of autocorrelation is considered to illustrate how the DCUSUM and DCCUSUM chart's detection performance is seriously affected due to presence of autocorrelation when detecting a range of process mean shifts.

Assume that $\{Y_t;\ \text{for } t \geq 1\}$ observations of quality characteristic of the ongoing process follow a standard normal distribution with the process parameters $\mu_Y = 0$ and $\sigma_Y = 1$. It is supposable that this process stays in the IC state for $t \leq t_0$; however, when $t > t_0$, this process goes OC due to an upward shift in the IC process mean $\mu_Y = 0$ with the value of $\delta = 0.5$. For the sake of brevity, three different levels of autocorrelation are considered here: no autocorrelation ($\phi = 0.0$), moderate level of autocorrelation ($\phi = 0.5$) and high level of autocorrelation in process ($\phi = 0.9$). 70 samples were generated with the first 50 for in-control state Phase-I and the last 20 for OC Phase-II e.g., ($t_0 = 50, 20$). In order to detect shift in this process, the two-sided DCUSUM and DCCUSUM charts are applied to these data with the chart parameters ($k_1 = 0.72, k_2 = 1.91, h_1 = 3.9070, h_2 = 1.4728$) and ($k_1 = 0.72, k_2 = 1.91, h_1 = 3.8136, h_2 = 1.4376$), respectively. The IC ARLs of these two-sided dual CUSUM CCs are set to $\text{ARL}_0 = 500$ and are displayed in Figs. 11-13.

The above figures vividly explain the deteriorating powers of the two charts, with the gradual intensity of autocorrelation. When there is no autocorrelation at work, the DCUSUM and DCCUSUM initiate a signal at sample number 54 and 53. With 0.5 autocorrelation level, it becomes 61, 61, while 0.9 autocorrelation aggravates it further to 67 and 66.

## VI. CONCLUSION AND RECOMMENDATIONS

In this article, we have proposed the new DCUSUM and DCCUSUM charts for monitoring the mean of the autocorrelated processes using the AR(1) model. Monte-Carlo simulations are used to compute the sensitive performance run-length measures, ARL and SDRL, for both zero-state and steady-state. In addition, to compute the overall performance of a chart for different size of shifts, we calculated EQL, RARL, and PCI. These measures have shown that the autocorrelation significantly affected the performance of the DCUSUM and DCCUSUM charts. To reduce this adverse effect, it could be used by s-skipping sampling as a redial measure. By comparing the two charts, it is found that the DCCUSUM is slightly more efficient as compared to the DCUSUM chart. Thus, the DCCUSUM chart is recommended for efficiently monitoring the autocorrelated process mean.

Since this study assuming that the process parameters are known, for future research works, it is possible to extend the research for estimated parameters. Moreover, as we considered the AR(1) model for the autocorrelation, the study can also be prolonged for other time series processes, such as AR(p) with p>1.

## ACKNOWLEDGMENT

The authors would like to thank all faculty and staff of the School of Statistics, Shanxi University of Finance and Economics, for their kind support in Covid-19 pandemic.

## CONFLICT OF INTEREST & DISCLOSURE

The authors declare that they have no conflicts of interest to report regarding the present study.

## REFERENCES

[1] D. C. Montgomery, *Introduction to Statistical Quality Control*, 6th ed. New York, NY, USA: Wiley, 2009.
[2] W. A. Shewhart, *Economic Control of Quality of Manufactured Product*. London, U.K.: Macmillan, 1931.
[3] A. R. Kamat, "Continuous inspection schemes," *Biometrika*, vol. 41, nos. 1–2, pp. 100–115, Apr. 1954.
[4] S. W. Roberts, "Control chart tests based on geometric moving averages," *Technometrics*, vol. 1, pp. 239–250, Aug. 1959.
[5] R. B. Crosier, "A new two-sided cumulative sum quality control scheme," *Technometrics*, vol. 28, no. 3, pp. 187–194, Aug. 1986.
[6] J. M. Lucas, "Combined Shewhart-CUSUM quality control schemes," *J. Qual. Technol.*, vol. 14, no. 2, pp. 51–59, Apr. 1982.
[7] M. Klein, "Composite Shewhart-EWMA statistical control schemes," *IIE Trans.*, vol. 28, no. 6, pp. 475–481, Jun. 1996.
[8] J. M. Lucas and R. B. Crosier, "Fast initial response for CUSUM quality control schemes: Give your CUSUM a head start," *Technometrics*, vol. 24, no. 3, pp. 205–1990, Aug. 1982.
[9] S. H. Steiner, "EWMA control charts with time-varying control limits and fast initial response," *J. Quality Technol.*, vol. 31, no. 1, pp. 75–86, Jan. 1999.
[10] Y. Zhao, F. Tsung, and Z. Wang, "Dual CUSUM control schemes for detecting a range of mean shifts," *IIE Trans.*, vol. 37, no. 11, pp. 1047–1057, Nov. 2005.
[11] A. Haq and L. Bibi, "A new dual CUSUM mean chart," *Qual. Rel. Eng. Int.*, vol. 35, no. 4, pp. 1245–1262, Jun. 2019.
[12] L. Liu, J. Zhang, and X. Zi, "Dual nonparametric CUSUM control chart based on ranks," *Commun. Statist.-Simul. Comput.*, vol. 44, no. 3, pp. 756–772, Mar. 2015.
[13] N. Abbas, I. A. Raji, M. Riaz, and K. Al-Ghamdi, "On designing mixed EWMA dual-CUSUM chart with applications in petro-chemical industry," *IEEE Access*, vol. 6, pp. 78931–78946, 2018.
[14] I. A. Raji, M. Riaz, and N. Abbas, "Robust dual-CUSUM control charts for contaminated processes," *Commun. Statist.-Simul. Comput.*, vol. 48, no. 7, pp. 2177–2190, Aug. 2019.
[15] A. Haq and L. Bibi, "The dual CUSUM charts with auxiliary information for process mean," *Commun. Statist.-Simul. Comput.*, vol. 51, no. 1, pp. 164–189, Jan. 2022.

[16] A. F. B. Costa and P. Castagliola, "Effect of measurement error and autocorrelation on the $X^{-}$ chart," *J. Appl. Statist.*, vol. 38, no. 4, pp. 661–673, Apr. 2011.

[17] C.-W. Lu and M. Reynolds, Jr., "EWMA control charts for monitoring the mean of autocorrelated processes," *J. Qual. Technol.*, vol. 31, no. 2, pp. 166–188, 2018.

[18] O. O. Atienza, L. C. Tang, and B. W. Ang, "Simultaneous monitoring of sample and group autocorrelations," *Qual. Eng.*, vol. 14, no. 3, pp. 489–499, Mar. 2002.

[19] R. Osei-Aning, S. A. Abbasi, and M. Riaz, "Mixed EWMA-CUSUM and mixed CUSUM-EWMA modified control charts for monitoring first order autoregressive processes," *Qual. Technol. Quant. Manage.*, vol. 14, no. 4, pp. 429–453, Oct. 2017.

[20] O. Y. E. Albarracin, A. P. Alencar, and L. L. Ho, "Effect of neglecting autocorrelation in regression EWMA charts for monitoring count time series," *Qual. Rel. Eng. Int.*, vol. 34, no. 8, pp. 1752–1762, Dec. 2018.

[21] P. Qiu, W. Li, and J. Li, "A new process control chart for monitoring short-range serially correlated data," *Technometrics*, vol. 62, no. 1, pp. 71–83, Jan. 2020.

[22] V. W. Lirio, T. Martins, B. Reichert, G. S. W. Lirio, A. M. Souza, and W. V. da Silva, "Literature review on control charts for autocorrelated processes," *Ciência e Natura*, vol. 44, p. e2, Mar. 2022.

[23] M. Anastasopoulou and A. C. Rakitzis, "EWMA control charts for monitoring correlated counts with finite range," *J. Appl. Statist.*, vol. 49, no. 3, pp. 553–573, Feb. 2022.

[24] S. Jafarian-Namin, M. S. Fallahnezhad, R. Tavakkoli-Moghaddam, and A. Salmasnia, "Desensitized control charts with operational importance for autocorrelated processes," *Qual. Technol. Quantum Manage.*, vol. 19, no. 6, pp. 665–691, 2022.

[25] S.-N. Lin, C.-Y. Chou, S.-L. Wang, and H.-R. Liu, "Economic design of autoregressive moving average control chart using genetic algorithms," *Expert Syst. Appl.*, vol. 39, no. 2, pp. 1793–1798, Feb. 2012.

[26] S. Bisgaard and M. Kulahci, "Quality quandaries: The effect of autocorrelation on statistical process control procedures," *Qual. Eng.*, vol. 17, no. 3, pp. 481–489, Jul. 2005.

[27] D. A. Nembhard and H. B. Nembhard, "A demerits control chart for autocorrelated data," *Qual. Eng.*, vol. 13, no. 2, pp. 179–190, Dec. 2000.

[28] C.-W. Lu and M. R. Reynolds, "CUSUM charts for monitoring an autocorrelated process," *J. Qual. Technol.*, vol. 33, no. 3, pp. 316–334, Jul. 2001.

[29] S. Knoth and W. Schmid, "Control charts for time series: A review," *Frontiers Stat. Qual. Control*, vol. 7, no. 2004, pp. 210–236, 2004.

[30] S. Psarakis and G. E. A. Papaleonida, "SPC procedures for monitoring autocorrelated processes," *Qual. Technol. Quant. Manage.*, vol. 4, no. 4, pp. 501–540, Jan. 2007.

[31] D. R. Prajapati and S. Singh, "Control charts for monitoring the autocorrelated process parameters: A literature review," *Int. J. Productiv. Quality Manage.*, vol. 10, no. 2, pp. 207–249, 2012.

[32] L. C. Alwan and D. Radson, "Time-series investigation of subsample mean chart," *IIE Trans.*, vol. 24, no. 5, pp. 66–80, Nov. 1992.

[33] K. C. Gilbert, K. Kirby, and C. R. Hild, "Charting autocorrelated data: Gltidelines for practitioners," *Qual. Eng.*, vol. 9, no. 3, pp. 367–382, Jan. 1997.

[34] Z. Wu, M. Yang, W. Jiang, and M. B. C. Khoo, "Optimization designs of the combined Shewhart-CUSUM control charts," *Comput. Statist. Data Anal.*, vol. 53, no. 2, pp. 496–506, Dec. 2008.

[35] S. Ahmad, S. A. Abbasi, M. Riaz, and N. Abbas, "On efficient use of auxiliary information for control charting in SPC," *Comput. Ind. Eng.*, vol. 67, pp. 173–184, Jan. 2014.


**YI LI** is currently working as an Associate Professor with the Statistics of School, Shanxi University of Finance and Economics. His research interests include machine learning, data mining and applied statistics, text mining, and sampling survey.

**TAHIR MUNIR** received the B.S. degree (Hons.) in statistics from Bahauddin Zakariya University, Pakistan, in 2015, and the M.Phil. degree in statistics from the Department of Statistics, Quaid-i-Azam University, Islamabad, Pakistan, in 2019. He has been working as a Research Specialist at The Agha Khan University, Karachi, Pakistan, since 2021. His research interests include the field of statistical process control, biostatistics, and machine learning.

**XUELONG HU** received the Ph.D. degree in control science and engineering from NUST, in 2016. He is currently an Associate Professor with the School of Management, Nanjing University of Posts and Telecommunications. His research interests include the new statistical quality monitoring and active queue management.